

**IMPACT OF BIODEGRADABLE MATERIALS ON
HEALTHY AND DISEASED BRAIN CELLS:
FUNCTION AND VIABILITY**

by

Kyle Mason Rugg, B.S. of Chemistry

A Thesis Presented in Partial Fulfillment
of the Requirements for the Degree
Masters of Science

COLLEGE OF ENGINEERING AND SCIENCE
LOUISIANA TECH UNIVERSITY

February 2022

LOUISIANA TECH UNIVERSITY

GRADUATE SCHOOL

October 22, 2021

Date of thesis defense

We hereby recommend that the thesis prepared by

Kyle Mason Rugg B.S.

entitled **IMPACT OF BIODEGRADABLE MATERIALS ON**
HEALTHY AND DISEASED BRAIN CELLS: FUNCTION AND
VIABILITY

be accepted in partial fulfillment of the requirements for the degree of

Master of Science in Molecular Sciences and Nanotechnology



Dr. Mark A DeCoster
Supervisor of Thesis Research

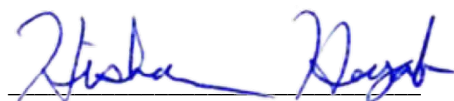


Dr. Gergana Nestorova
Head of Molecular Sciences and Nanotechnology

Thesis Committee Members:

Dr. Mark DeCoster
Dr. Bryant Hollins
Dr. Gergana Nestorova

Approved:



Hisham Hegab
Dean of Engineering & Science

Approved:



Ramu Ramachandran
Dean of the Graduate School

ABSTRACT

With the recent creation of Metal Organic Biohybrids (MOBs) from the DeCoster lab group at Louisiana Tech University, a new class of nano and micro particles needs to be investigated. The amalgamation of metals such as copper and an amino acid have already shown promise for biomedical applications such as delayed drug delivery or time delayed anti-microbial effects¹. In this study the effects of cobalt, copper, and zinc-based MOBs have been compared against silicon dioxide nanoparticles, a negative control, and copper oxide nanoparticles, a positive control, in order to observe their effects on cancerous glioma cells and healthy astrocyte cells. The cellular health was examined in terms of cell metabolism, calcium response intensity and nuclear morphology via MTT assay, DAPI staining and calcium imaging.

The study showed that all MOBs tested had desired negative effects on both the astrocyte and glioma cell lines. Of exception were CuHARs which were able to successfully decrease the astrocyte metabolism by 21% and the glioma was more harshly affected at 29%. Calcium imaging data of glioma also showed an initial suppression followed by agitation concluded by suppression when compared to control cells. When CuHARs were compared to CuNPs by concentration of copper mass present in the total dose of the material. the metabolism was $89 \pm 0\%$ CuNPs and $94 \pm 0\%$ CuHARs at 24Hrs. In summary, all MOBs tested showed promise and with alterations to dosages, amounts, and loadings they may be a key to a new cancer treatment method.

APPROVAL FOR SCHOLARLY DISSEMINATION

The author grants to the Prescott Memorial Library of Louisiana Tech University the right to reproduce, by appropriate methods, upon request, any or all portions of this Thesis. It is understood that “proper request” consists of the agreement, on the part of the requesting party, that said reproduction is for his personal use and that subsequent reproduction will not occur without written approval of the author of this Thesis. Further, any portions of the Thesis used in books, papers, and other works must be appropriately referenced to this Thesis.

Finally, the author of this Thesis reserves the right to publish freely, in the literature, at any time, any or all portions of this Thesis.

Author _____

Date _____

DEDICATION

This work is dedicated to my mother, without whose support, I am sure I would not have made it this far, to my advisor Dr. Mark A. DeCoster who has guided me for a quarter of my life, since before my first day of undergraduate, into the scientist and man I would become, and finally, my to The Lord God Almighty who has shown me all things are possible in His name.

TABLE OF CONTENTS

ABSTRACT	iii
APPROVAL FOR SCHOLARLY DISSEMINATION	v
DEDICATION	vi
LIST OF FIGURES	ix
LIST OF TABLES	xii
ACKNOWLEDGEMENTS.....	xiii
CHAPTER 1 INTRODUCTION.....	1
1.1 Nanoparticles and Metal Organic Biohybrids.....	1
1.2 Research Objectives.....	4
CHAPTER 2 METHODOLOGY.....	6
2.1 Copper Nanoparticles.....	6
2.2 Copper MOBs (CuHARs)	7
2.2.1 Proposed CuHARs Structures	7
2.3 Zinc MOBs	10
2.4 Cobalt MOBs	11
2.5 Silicon Dioxide Nanoparticles.....	12
2.6 Cell Culture and Addition of Materials.....	13
2.7 MTT Assay.....	16
2.8 Digital Microscopy.....	17

2.9	Calcium Imaging.....	17
2.10	DAPI Staining	19
2.11	Image Analysis and Data Normalization.....	20
CHAPTER 3 RESULTS.....		24
3.1	Cobalt MOBs.....	25
3.1.1	Cobalt MOBs Impact on Cell Metabolism.....	25
3.1.2	Cobalt MOBs Impact on Cell Morphology.....	26
3.1.3	Cobalt MOBs Impact on Cell Response.....	29
3.2	CuHARs.....	30
3.2.1	CuHARs Impact on Cell Metabolism.....	30
3.2.2	CuHARs Impact on Cell Morphology.....	32
3.2.3	CuHARs Impact on Cell Response.....	34
3.3	Zinc MOBs.....	35
3.3.1	Zinc MOBs Impact on Cell Metabolism.....	35
3.3.2	Zinc MOBs Impact on Cell Morphology.....	37
3.3.3	Zinc MOBs Impact on Cell Response.....	39
3.4	Silicon Dioxide NPS.....	41
3.4.1	Silicon Dioxide NPS Impact on Cell Metabolism.....	41
3.4.2	Silicon Dioxide NPS Impact on Cell Morphology.....	41
3.4.3	Silicon Dioxide NPS Impact on Cell Response.....	43
3.5	Copper Nanoparticles	44
3.5.1	CuNPs Impact on Cell Metabolism.....	44
3.5.2	CuNPs Impact on Cell Morphology.....	45

3.5.3	CuNPs Impact on Cell Response.....	48
CHAPTER 4 DISCUSSION.....		49
4.1	The Impact of Cobalt MOBs on Cells.....	50
4.2	The Impact of CuHARs on Cells.....	51
4.3	The Impact of Zinc MOBs on Cells.....	53
4.4	The Impact of Silicon Dioxide Nanoparticles on Cells.....	54
4.5	The Impact of Copper Nanoparticles on Cells.....	55
CHAPTER 5 CONCLUSIONS AND FUTURE WORKS.....		57
5.1	Conclusions.....	57
5.2	Future Works.....	59
APPENDIX A	Astrocyte Culture Media.....	62
APPENDIX B	CRL-2303 Culture Media.....	63
APPENDIX C	Poly-L-Lysine Protocol.....	64
APPENDIX D	DAPI Staining Protocol.....	65
APPENDIX E	MTT Assay for Astrocytes and CRL-2303	66
APPENDIX F	Standard 7.0ml Synthesis of MOBs.....	67
BIBLIOGRAPHY.....		68

LIST OF FIGURES

Figure 2-1-1: Vortexed CuNPs stock solution 2mg/ml.	6
Figure 2-2-1: Copper (I) oxide (left) and copper (II) oxide (right), a nanoparticle starting reagent used in synthesis of CuHARs (product).	8
Figure 2-2-2: Cystine starting reagent used for synthesis.	8
Figure 2-2-3: Cystine central copper superimposition of cystine, possible product structure.....	9
Figure 2-2-4: Cystine capped copper structure of cystine, possible product structure.	9
Figure 2-2-5: Cystine chain with copper R groups, possible product structure.....	10
Figure 2-3-1: Freshly collected zinc MOB synthesis product in a 15ml tube. Approximate mass of 0.28mg (left) and 0.21mg (right).	11
Figure 2-4-1: Successful synthesis product liquid of Co MOBs in suspension.	12
Figure 2-5-1: Silicon dioxide nanoparticles in suspension.	13
Figure 2-6-1: Standard example of a cell culture plate of astrocytes mid-growth period being observed as a part of standard care. No materials have been added, and the surrounding wells can be seen containing water to prevent dry outs.	15
Figure 2-6-2: 400µg/ml dilutions of materials and astrocyte media waiting to be added to the cultures. These materials were mixed and refrigerated approx. 24hrs. before photographing to allow some comparisons of settling to be shown.	16
Figure 2-7-1: A plate of astrocytes being prepared for MTT assay with 500µl of iso-2-propanol alcohol added to dissolve the formazan crystals. Visual comparisons can be made of different conditions at this time directly after the addition of alcohol. For example, the second column labeled CuNPs has a distinctly less purple hue than the controls of zinc MOB areas.	17

Figure 2-9-1: View above a phase light image from a calcium imaging session merged with a pseudo-color image of the same frame to indicate intensity of response. This frame was taken after the addition of Ionomycin, a positive control showing maximum response.	19
Figure 2-10-1: View above (left) glioma cells grown 5 DIV, and (right) a DAPI stain of the same view. Note the variety of cell sizes and elongated transparent nature of the cell body and processes, indicating healthy adhesion to the flask. Cells also lack a “halo” effect that may come from a cell becoming round as it lifts off the surface, causing light to bend.	20
Figure 3-1-1: The above image (left) is a phase light image of Cobalt MOBs 48hrs. exposure and (right) a DAPI stain of glioma cells grown 5 DIV, fixed, and then stained to image. Note the larger-than-normal nuclei that were present in some Co MOB cultures.	27
Figure 3-1-2: The above image (left) is a phase light image of Cobalt MOBs 48hrs. exposure and (right) a DAPI stain of astrocyte cells grown 5 DIV, fixed, and then stained to image. Note the larger-than-normal nuclei that were present in some Co MOB cultures..	28
Figure 3-1-3: In the figure above, we see the calcium response data for glioma cells exposed to cobalt MOBs 24 and 48 hrs., compared with a control well with no additions.	29
Figure 3-2-1: The above image (left) is a phase light image of CuHARs 48hrs. exposure and (right) a DAPI stain of glioma cells grown 5 DIV, fixed, and then stained to image.	32
Figure 3-2-2: The above image (left) is a phase light image of CuHARs 48hrs. exposure and (right) was a DAPI stain of astrocyte cells grown 5 DIV, fixed, and then stained to image.	33
Figure 3-2-3: In the figure above, we see the calcium response data for glioma cells exposed to CuHARs MOBs 24 and 48 hrs., compared with a control well with no additions.....	34
Figure 3-3-1: The above image (left) is a phase light and (right) a DAPI stain of glioma cells grown 5 DIV, exposed to zinc MOBs for 48hrs., fixed, and then stained to image.	37
Figure 3-3-2: The above image (left) is a phase light and (right) a DAPI stain of astrocyte cells grown 5 DIV, exposed to zinc MOBs for 48hrs., fixed, and then stained to image.	38
Figure 3-3-3: In the figure above, we see the calcium response data for glioma cells exposed to zinc MOBs 24 and 48 hrs., compared with a control well with no additions. Note the stress peaks in the 48hrs. group and lack of response from the 24hrs. group.	39

- Figure 3-4-1:** The above image (left) is a phase light image of SiO₂ nanoparticles 24hrs. exposure and (right) a DAPI stain of glioma cells grown 5 DIV, fixed, and then stained to image. Note the diversity of cell size and transparent bodies sans “halo.”.....42
- Figure 3-4-2:** The above image (left) is a phase light image of SiO₂ nanoparticles 24hrs. exposure and (right) a DAPI stain of astrocyte cells grown 5 DIV, fixed, and then stained to image. Note the diversity of cell size and transparent bodies sans “halo.”43
- Figure 3-4-3:** In the figure above, we see the calcium response data for glioma cells exposed to silicon dioxide nanoparticles 24 and 48 hrs., compared with a control well with no additions.44
- Figure 3-5-1:** The above image (left) is a phase light image of CuNPs 24hrs. exposure and (right) a DAPI stain of glioma cells grown 5 DIV, fixed, and then stained to image. Note the smaller, round cell bodies and “halo” effect around objects indicating lift.46
- Figure 3-5-2:** The above image (left) is a phase light image of CuNPs 24hrs. exposure and (right) a DAPI stain of astrocyte cells grown 5 DIV, fixed, and then stained to image. Note the smaller, round cell bodies and “halo” effect around objects indicating lift.47
- Figure 3-5-3:** In the figure above, we see the calcium response data for glioma cells exposed to copper nanoparticles 24 and 48 hrs., compared with a control well with no additions. Note the rapid response of the 48hrs. group and the high intensity peak, indicating stress.48

LIST OF TABLES

Table 3-1-1: Cobalt MOBs glioma MTT data.	25
Table 3-1-2: Cobalt MOBs astrocyte MTT data.	26
Table 3-1-3: Cobalt MOBs glioma DAPI data.	27
Table 3-1-4: Cobalt MOBs astrocyte DAPI data.	28
Table 3-2-1: CuHARs glioma MTT data.	30
Table 3-2-2: CuHARs astrocyte MTT data.	31
Table 3-2-3: CuHARs glioma DAPI data.	32
Table 3-2-4: CuHARs astrocyte DAPI data.	33
Table 3-3-1: Zinc MOBs glioma MTT data.	35
Table 3-3-2: Zinc MOBs astrocyte MTT data.	36
Table 3-3-3: Zinc MOBs glioma DAPI data.	37
Table 3-3-4: Zinc MOBs astrocyte DAPI data.....	38
Table 3-4-1: Silicon dioxide nanoparticles glioma MTT data.	40
Table 3-4-2: Silicon dioxide nanoparticles astrocyte MTT data.	41
Table 3-4-3: Silicon dioxide nanoparticles glioma DAPI data.	42
Table 3-4-4: Silicon dioxide nanoparticles astrocyte DAPI data.	43
Table 3-5-1: CuNPs 10µg/ml vs CuHARs 20µg/ml astrocyte MTT data.	45
Table 3-5-2: CuNPs glioma DAPI data.	46
Table 3-5-3: CuNPs astrocyte DAPI data.	47
Table 4-1-1: In the table we see a summary of major qualities of each material on cells.	53

ACKNOWLEDGMENTS

Firstly, I would like to thank my advisor Dr. Mark DeCoster. He has guided me since I stumbled into his office back in 2015 wanting to know his “specialty”, and somehow miraculously asked me to join his lab. He, for 7 years now has invested much more than just scientific knowledge, scholarly traits and what it takes to be successful in academia but has also shown me how to lead life.

My colleague, friend, and mentor Elnaz Khezlou made a large majority of this work possible. She was there to show me, right as Covid-19 struck, how to perform calcium imaging by myself and continually train me in cell culture. She was also instrumental in astrocyte culture in the latter half of this work and provided guidance and insight on materials and stimulus effects on cells.

Navya Uppu, a close friend and fellow researcher, was always eager to assist me in my endeavors. She was there to provide answers when she had them and never failed to join me in search of them when she did not.

My dear friends and past members of the lab Muhetaer Tuerhong, Anik Karan and Zach Norcross deserve more gratitude than I can express. While I might not have understood their work in the moment, I certainly today stand on their shoulders today as they paved the way of these materials.

Lastly, I would like to thank my mother Angela Rugg and father Jeff Rugg. Without their support I would have not had the strength to continue through the many trials of life. They were always there for me, through the thousands of phone calls listing off random chemicals, explaining my day, or asking for life advice.

CHAPTER 1

INTRODUCTION

1.1 Nanoparticles and Metal Organic Biohybrids (MOBs)

In the field of nanomedicine, we often look to the human body for inspiration.

There's often a pre-existing solution to a problem, and our duty is to study and replicate those functions with artificial means to improve health and quality of life. One such method of replicating these mechanisms is doped nanoparticles. Doped nanoparticles are small, easily manipulable, and full of potential². In the medical field, researchers have experimented with these particles by: loading them with drugs, tracking their movement, and guiding them to a final resting spot in the body. Their industrial applications range from beauty products, industrial chemistry, and oil drilling³, to medicine. With dimensions ranging of 100nm in diameter and smaller, their reactive surface area is higher per mass and volume than a more macro counter part⁴, and is more susceptible to chemical, magnetic manipulation, and sonic influences. The addition of a simple nanoparticle such as raw copper or silver nanoparticles⁵, while retaining their antimicrobial properties, can be so toxic to normal healthy tissue it is a challenge to utilize them⁶. However, with the advent of Metal Organic Biohybrids (MOBs)⁷, a particle created by the synthesis of an amino acid such as cysteine and a metal (copper, cobalt or zinc for example), one can reduce the toxic effects and possibly provide a new method of treatment for cancer¹.

Copper nanoparticles (CuNPs) are copper only materials with a size of 1-100nm in diameter. They can be made from a vast array of copper-based compounds, either from lab reagents or biologically⁸. Due to the range of manufacturing methods and copper's natural abundance, they are cheap and relatively easy to make. CuNPs are used in chemistry as a catalyst, preferred for their high surface area, and also have uses in other fields such as the production of dyes and biocides. This last entry is due to their toxic nature, and the toxic effects are dependent upon concentration⁹. In this study, CuNPs were selected as a positive control for their known toxic effects in cell culture.

Copper High Aspect Ratio Structures (CuHARS) are a unique class of MOB as standard MOB synthesis produces a roughly spherical product. CuHARS' synthesis, however, form long rod-like structures ranging from nanometers to a few hundred microns in length and maxes at 10 microns in width; hence high aspect ratio. These materials have already been successfully incorporated in cellulose bandages for controlled degradation, wound healing, and are desired for their antimicrobial properties¹. CuHARs are synthesized in accordance to the directions in Appendix F and made from CuSO_4 obtained from Sigma-Aldrich (St. Louis, MO, USA). Although, CuNPs can be substituted. In this study, CuHARs will be directly compared to the non-biological CuNPs. It is hypothesized that by mass of copper present, CuHARs compared to CuNPs would have a less toxic effect due to the reduced surface area slowing down the reaction kinetics and prolonging the exposure of copper-based dosing over a longer period of time at a lower dose. This may be desirable for medical applications.

Cobalt MOBs (Co MOBs) are made by combining cobalt (II or III) oxide nano powder with the amino acid cysteine at 37°C, both obtained from Sigma-Aldrich (St. Louis, MO, USA), in accordance with the standard synthesis prescribed in Appendix F. These products are novel and were created in our lab in July of 2021. Cobalt nanoparticles, however, have been used in medical tracking in MRI contrast solution¹⁰, and in an array of magnetic based biosensors¹¹. They also have been used for studying applications in cytotoxicity which show that they increase the presence of apoptotic reactions in human embryonic kidney cells, and have possible applications in cancer treatments¹². It is hypothesized that cobalt MOBs will have a less toxic effect than CuNPs due to the reduced surface area of the particle. However, they will have a more toxic effect than the CuHARs due to a higher charge of free cobalt ions compared to free copper ions once the MOB breaks down.

Zinc MOBs are made by combining $ZnSO_4 \cdot 7H_2O$, obtained from Sigma-Aldrich (St. Louis, MO, USA), with the amino acid cystine in accordance with the standard synthesis prescribed in Appendix F. Zinc oxide nanoparticles have been studied for their role as a cytotoxic agent¹². It is hypothesized that there may be similar damage to the cells from Zinc MOBs compared to the CuHARs due to a similar free ion charge (+2).

Silicon dioxide nanoparticles were selected in this study for their known non-biodegradable, inert qualities in cell culture. They are studied for their porous nature which makes them natural drug delivery devices^{13,14}. In this study, they will serve as a control for the presence of a chemically unreactive and non-biodegradable object; simply taking up space. I hypothesize that due to silicon dioxide's inert nature and zero charge,

the particles will have no discernable effect on the cell's health aside from a slight slowing in development due to the particles occupying free space.

In summary, each of these nanoparticles possess a possible solution to a vast array of issues. In this study, we are primarily looking at their effects on brain cells and their possible uses to selectively treat or detect glioma cells without severe consequences to the normal astrocyte cells¹⁵. The effects of each nanoparticle are caused by the metal substrates emitted as the materials degrade. They may share a common size and set of features, but their influences on cells will entirely be determined on their base metal and their organic constituent. It is hypothesized that a metal-based nanoparticle will have the most detrimental effects on a cell culture, followed by more mild effects from an MOB, and lastly a nearly unaffected culture with silicon dioxide particles.

1.2 Research Objectives

Throughout this work, there will be a few key points of interest for observation, listed below as research objectives. These will not be the only observations made, but serve as the driving questions to guided this work.

1. Study the effects of novel nanomaterials interacting with astrocyte and glioma cells. This research will primarily focus on copper nanoparticles (CuNPs), silicon dioxide nanoparticles (SiO₂), and copper-based MOBs (often known as CuHARS), zinc (Zn MOBs), and cobalt (Co MOBs) on healthy and diseased brain cells. Their effects will be characterized via cellular metabolism, calcium response to stimulus, and cell morphology.
2. Compare the toxicity effects of nano particles to biological MOBs.

- 2.A) Compare the toxicity effects of materials on glioma and astrocytes via MTT assay.
- 2.B) Compare the toxicity effects of materials on glioma and astrocytes via nuclear DAPI staining and computer aided examination of nuclear morphology.
3. Examine the acute effect of materials on the glioma cell's ability to respond to environmental stimulus utilizing calcium imaging.

CHAPTER 2

METHODOLOGY

2.1 Copper Nanoparticles

Copper nanoparticles are an industry standard for cytotoxic effects and are commonly implemented for antimicrobial properties^{16,17,18}. In this study, the CuNPs were obtained from an unrefrigerated stock solution of 2.0mg/ml in sterile water. The nanoparticles themselves were obtained from Sigma-Aldrich (St. Louis, MO, USA). The nanoparticles are a brown-black ink color in solution and will settle heavily, so sonication is needed before aliquoting, as shown below in Fig. 2-1-1. A solution of nanoparticles for cell culture was then made from this stock solution in the desired media for experiments.



Figure 2-1-1: Vortexed CuNPs stock solution 2mg/ml.

2.2 Copper MOBs (CuHARS)

CuHARS were synthesized by the standard procedure in Appendix F. Once the particles are synthesized, they must be spun down in a centrifuge at 2500 RFC, 10°C, in 20-minute intervals in a 15ml centrifuge tube. Once a pellet of product is formed at the bottom, all but the last 1.0ml of supernatant is removed and discarded. The last 1.0ml is then mixed with the pellet using a pipette-aid, and is then dried on a glass slide at 37°C. This was done to prevent decomposition. The dried product is then scraped using a razor blade and weighed, then either stored dry or at 1mg/ml in sterile water and refrigerated. The dried product should be light baby blue in color⁷. In solution, CuHARS will settle heavily, so sonication is needed before aliquoting. A solution of nanoparticles was then made from this in the desired media for cell culture.

2.2.1 Proposed CuHARS Structures

The following figures below are generated models of reagents and possible products of CuHARS synthesis. These models below were generated using the website MoleView.¹⁹ The model on the next page, Fig. 2-2-1 and subsequent models have red as oxygen and terracotta as copper. These copper oxides represent the CuNPs used in this study.

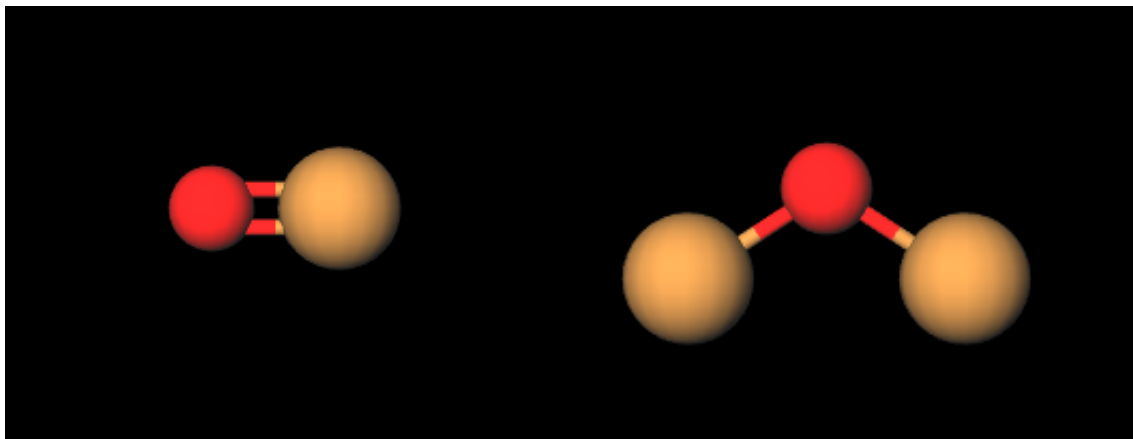


Figure 2-2-1: Copper (I) oxide (left) and copper (II) oxide (right), a nanoparticle starting reagent used in synthesis of CuHARs (product).

Next displayed Fig. 2-2-2, is the Cystine^{20,21} molecule, not to be confused with Cysteine, the former being an oxidized dimer of the latter's amino acid self-joined at the yellow sulfur.

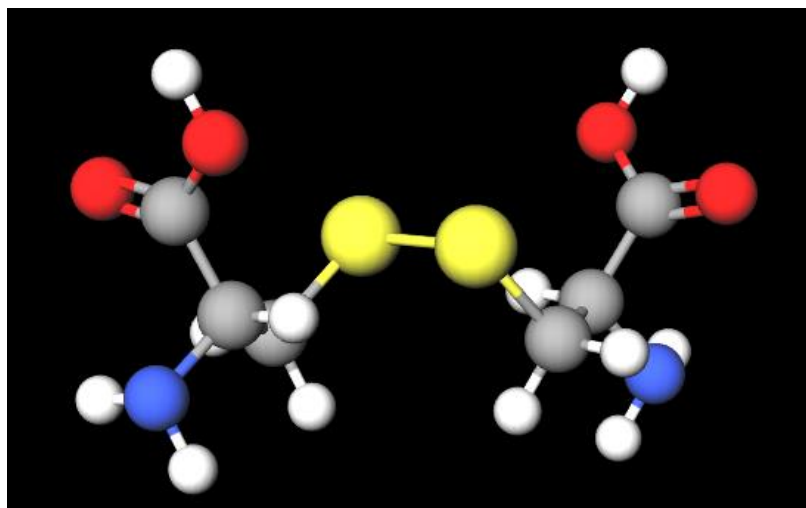


Figure 2-2-2: Cystine starting reagent used for synthesis.

First to be introduced, Fig 2-2-3, for possible products is this molecule where copper has super imposed itself in between the two amino acids²².

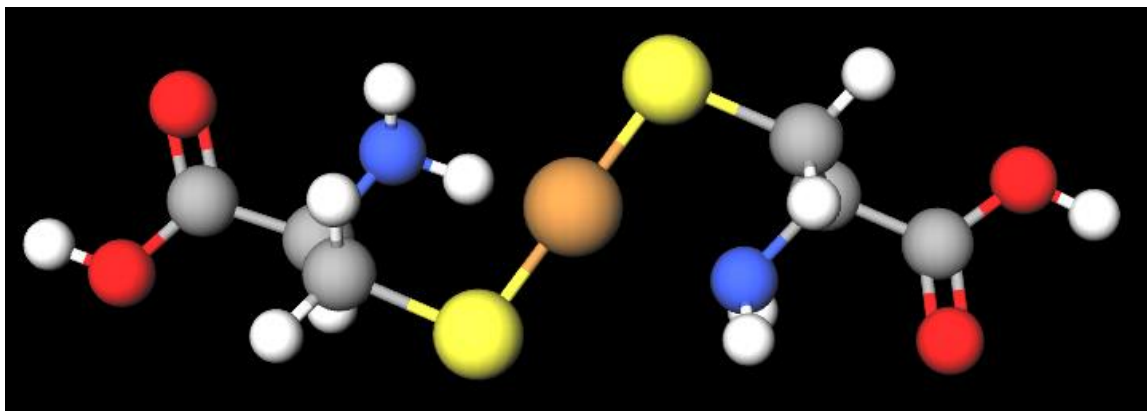


Figure 2-2-3: Cystine central copper superimposition of cystine, possible product structure. Note the linear aspect.

Next is a cystine molecule in Figure 2-2-4 which shows a copper capped cystine²³ possibly explain CuHARs limited width.

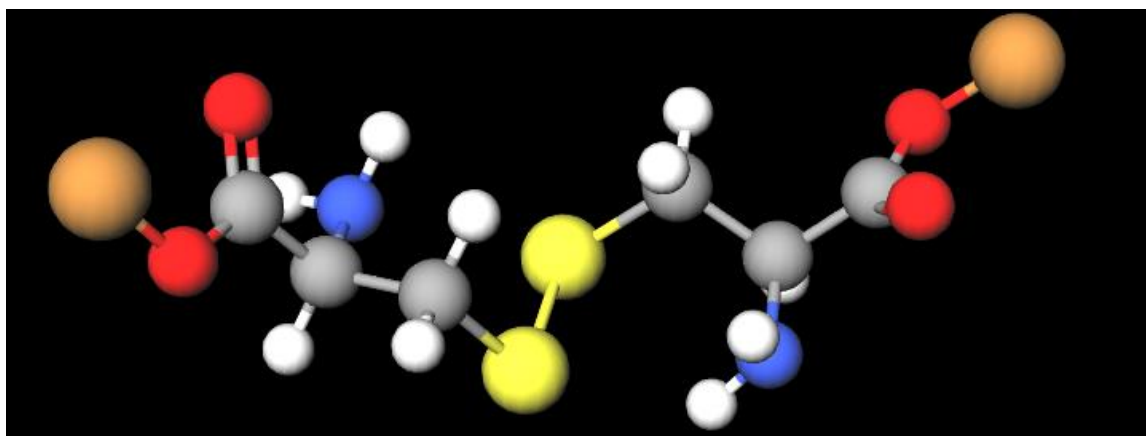


Figure 2-2-4: Cystine capped copper structure of cystine, possible product structure.

Lastly is the chain of cysteine amino acids capped with copper ions^{24,25}, Figure 2-2-5. This structure may explain CuHARs' length.

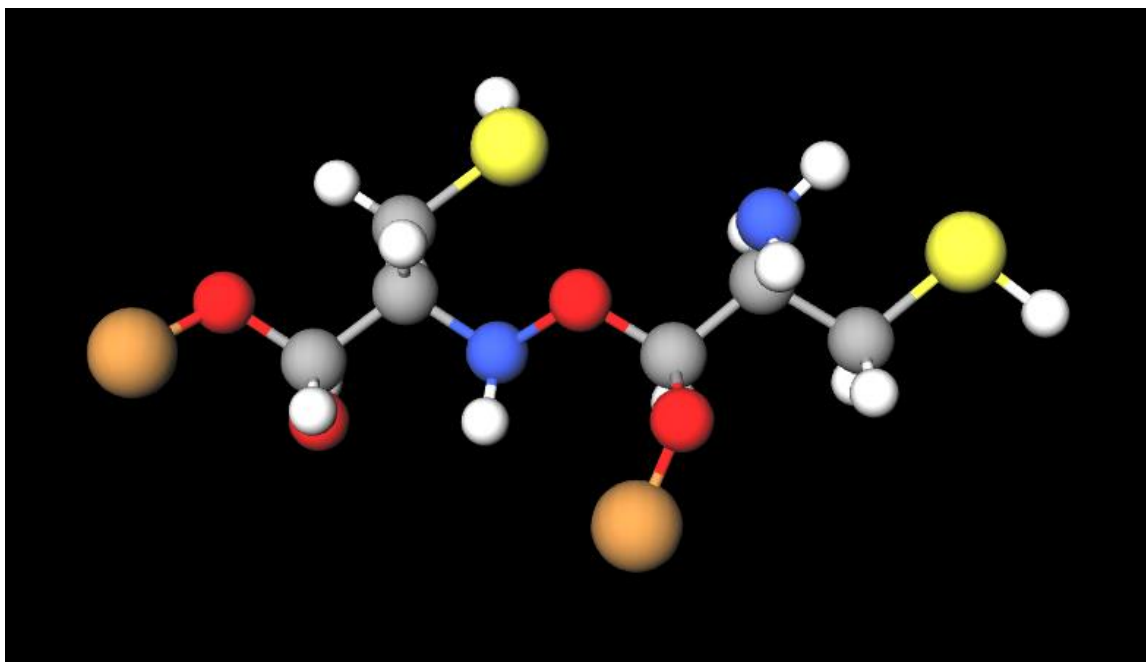


Figure 2-2-5: Cystine chain with copper R groups possible product structure.

2.3 Zinc MOBs

Zn MOBs were synthesized by the standard procedure in Appendix F. Once the particles are synthesized, they must be spun down in a centrifuge at 2500 RFC, 10°C in 20-minute intervals in a 15ml centrifuge tube. Once a pellet of product is formed at the bottom, all but the last 1.0ml of supernatant is removed and discarded. The last 1.0ml is then mixed with the pellet using a pipette-aid, and is then dried on a glass slide at 37°C. The dried product is then scraped using a razor blade and weighed, then either stored dry or at 1mg/ml in sterile water and refrigerated. In practice this method (7 ml synthesis, Appendix F) yields an average of 0.093 mg of product per synthesis, and if scaled up to triple the volume (21 ml flask synthesis), the yield is 0.07mg per 7ml synthesis. This shows that while loss occurs due to less favorable environments, scaling the synthesis is possible^{26, 27}. Zinc MOBs were stored in a 1mg/ml solution with sterile water and refrigerated. Zinc MOBs should have a white color in dried product, and in solution will

settle lightly, so vortexing/titration is needed before aliquoting. A solution of nanoparticles, as below in Figure 2-3-1, was then made from this in the desired media for experiments.

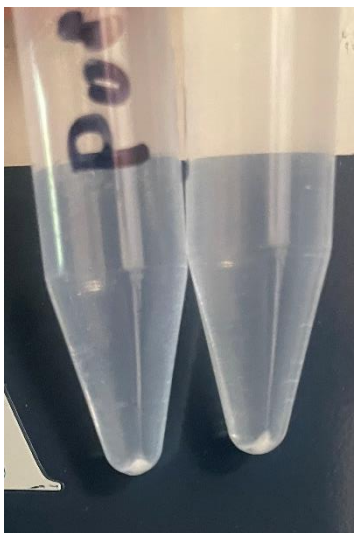


Figure 2-3-1: Freshly collected zinc MOB synthesis product in a 15ml tube. Approximate mass of 0.28mg left and 0.21mg right.

2.4 Cobalt MOBs

Co MOBs were synthesized by the standard procedure in Appendix F. Once the particles are synthesized, they must be spun down in a centrifuge at 2500 RFC, 10°C in 20-minute intervals in a 15ml centrifuge tube. Once a pellet of product is formed at the bottom, all but the last 1.0ml of supernatant is removed and discarded. The last 1.0ml is then mixed with the pellet using a pipette-aid, and is then dried on a glass slide at 37°C. The dried product is then scraped using a razor blade and weighed, then either stored dry or at 1mg/ml in sterile water and refrigerated. In practice according to Appendix F, 0.6 mg of product was achieved from a 41ml of synthesis across six batches of 7ml synthesis, yielding 0.08 mg of product per standard synthesis. In solution, as shown on the next page in Figure 2-4-1, the cobalt should have a distinct pale-yellow color²⁸ and will settle

mildly, so vortexing is needed before aliquoting. A solution of nanoparticles was then made from this in the desired media for cell culture.

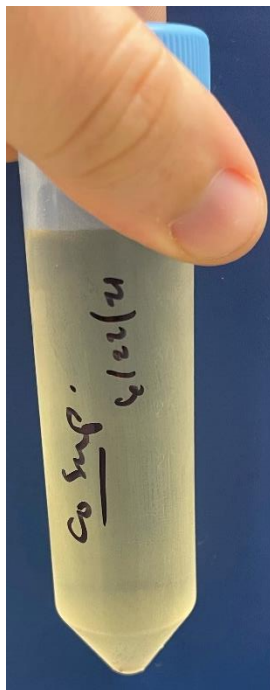


Figure 2-4-1: Successful synthesis product liquid of Co MOBs in suspension.

2.5 Silicon Nanoparticles

Silicon dioxide nanoparticles (5-15nm)¹⁴ were obtained from company Sigma-Aldrich (St. Louis, MO, USA), and then placed in a 2mg/ml solution with sterile water and refrigerated. In solution, the silicon nanoparticles should have a pale white color¹³ and will settle heavily, so vortexing is needed before aliquoting. A solution of nanoparticles, shown on the next page in Figure 2-5-1, was then made from this in the desired media for cell culture.



Figure 2-5-1: Silicon dioxide nanoparticles in suspension.

2.6 Cell Culture and Addition of Materials

In cell culture, 24 well cell culture plates, as shown in Figure 2-6-1, were used to culture astrocytes or glioma. The astrocytes were harvested from newborn rat pups, and the glioma were cell line CRL-2303 ATCC. From the center two rows, 10 wells were used to culture the cells and surrounding wells had sterile water added to prevent dry outs. For glioma cells, 1.0ml of media was added to each well and then placed in the incubator to warm. In the case of astrocytes, poly-L-lysine was added to the plates pre-addition of media as described in Appendix C. This addition is required to ensure the astrocytes have good adhesion to the plate²⁹. Once the plates are being warmed, cells were passaged from stock flasks used between passage 1-20^{30, 31.32} for glioma, and passage 1-7 for astrocytes. Cell flasks first have the media and dead cells removed via pipetting, and then 2.0ml of sterile PBS³³ 1X are added, and the flask gently swirled to

wash. The PBS is subsequently removed and then 1.5ml of trypsin EDTA³⁴ is added to the flasks, and then they are placed back in the incubator for 5 minutes. After the 5 minutes, the flasks are visually examined by holding them up to the light, looking for the free-floating cell sheets which are opaque with no remaining segments adhered to the flask. Once the cells are fully detached, the cells are pipetted into a 15ml conical tube along with 2ml of cell media and spun down in a centrifuge at 160 RCF for 8 minutes at 10°C. Once a cell pellet has been achieved the supernatant is removed and then 2.0ml of media is added back to the tube. The cells are then vortexed, and using a hemocytometer³⁵, the average cell density is recorded. The cells were plated at the desired density in each of the wells and in the flask, typically 5000 cells/ml of media³⁶.

Once a plate has had the addition of the cells, in the case of glioma, it will be 5-7 days until the cells are 100% confluent while astrocytes will take 7-9 days. Having a cell culture at approximately 90% confluence³⁷ is optimal as it allows for maximum cells in a field of view for microscopy that are still individually distinguishable. However, in terms of MTT assay confluence is still relative; but since it relies on cellular metabolism, as long as the cells have not diversified or grown in multi layered sheets, it is still utilizable in the 90-100% confluence range³⁸. The addition of materials in these experiments were added 24 or 48 hrs. prior to imaging or assays in final concentrations of 20ug/ml. For example, a plate of 10 wells with cells will have 2 wells with an addition of cell media, a negative control, and 2 wells with the addition of CuNPs as a positive control; one each at 24 and 48hrs. Lastly, 2 rows of 3 wells for the material of investigation, one set added at 24hrs. and one set added at 48 hrs. prior to experimentation (pictured next page Figure 2-6-1).

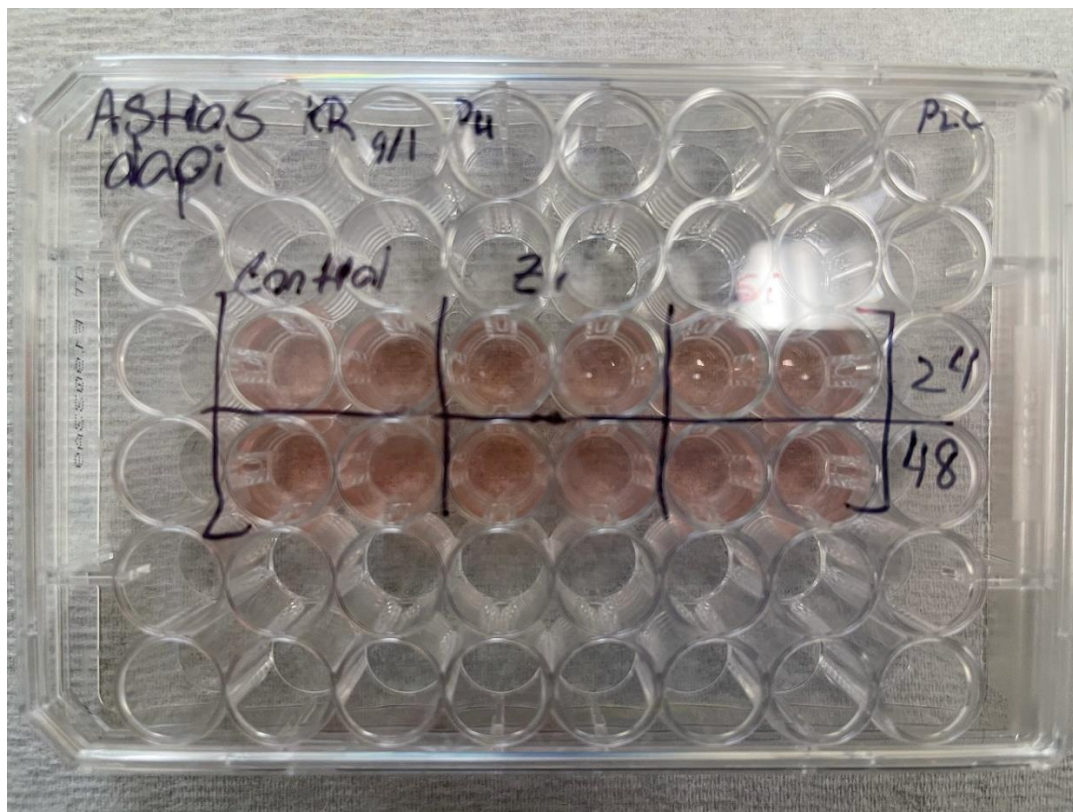


Figure 2-6-1: Standard example of a cell culture plate of astrocytes mid growth period being observed as part of standard care. No materials have been added and the surrounding wells can be seen containing sterile water to prevent dry outs.

Figure 2-6-2 was taken to show what most materials look like in suspension before addition to cell cultures, as these are materials about to be added for the 24hrs. group and have sat for 24hrs. approx. It also demonstrates that some material settles as shown in Figure 2-6-2 on the following page, most prominently displayed in the case of CuNPs.

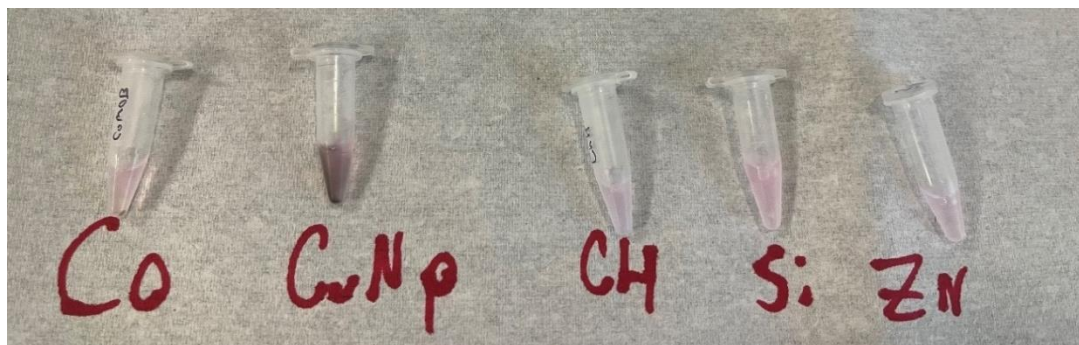


Figure 2-6-2: 400ug/ml dilutions of materials and astrocyte media waiting to be added to the cultures. These materials were mixed and refrigerated approx. 24hrs. before photographing to allow some comparisons of settling to be shown. Left to right: cobalt MOBs, copper nanoparticles, CuHARS, silicon dioxide nanoparticles and zinc MOBs.

2.7 MTT Assay

For MTT assay, a spectrophotometer was used in conjunction with the MTT powder obtained from Sigma-Aldrich (St. Louis, MO, USA) along with the cell culture plate. The protocol is written in Appendix E. The spectrophotometer used was a Genesys 20 from Thermo Spectronic, at 630nm for glioma and 570nm for astrocytes. The instrument was pre-warmed before use to avoid fluctuating bulb heat causing a drift in value. A max drift in absorbance value recorded in a 1hr. period of idle time was +/- 0.003.

The purpose of MTT assaying cell cultures, pictured on the following page in Figure 2-7-1, was to assess the cells' metabolism. The initial addition of yellow tetrazole is reduced to formazan purple by the cells^{39, 40, and 41}. The rate at which they are able to process this is determined by their metabolism. Therefore, an injured or negatively affected cell will not be able to metabolize as much tetrazole in 1hr as an otherwise unaffected cell.

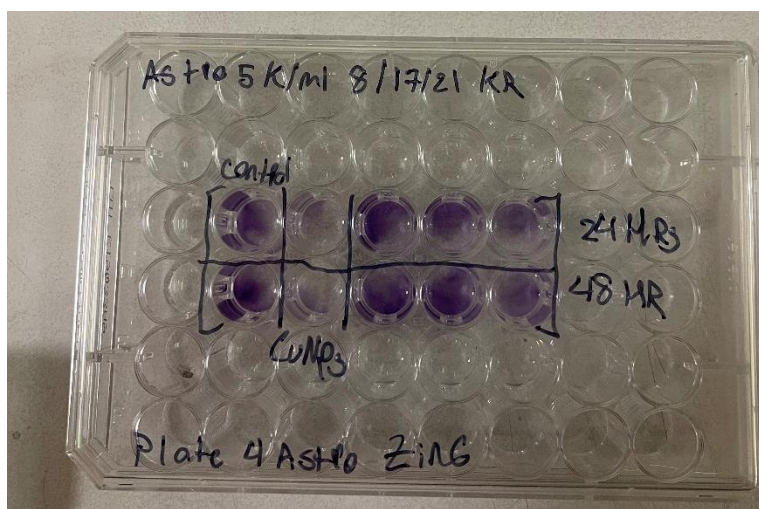


Figure 2-7-1: A plate of astrocytes being prepared for MTT assay with 500ul of iso2propanol alcohol added to dissolve the formazan crystals. Visual comparisons can be made of different conditions at this time directly after addition of alcohol. For example, the second column labeled CuNPs has a distinctly less purple hue than the controls of zinc MOB areas. (First column).

2.8 Digital Microscopy

The majority of the digital microscopy was performed on one of two stations; a Leica DMI 6000 B with light source Kubler Codix and powered by Leica software version 2.0 and run by a Windows 8 computer for DAPI staining. The other main station was an Olympus IX 51 inverted microscope with a light source Olympus TH4-100 for white light and Polychrome V for fluorescent light. This was run on a windows computer version 8 operating the program Incytam 1 for calcium imaging.

2.9 Calcium Imaging

For calcium imaging, the first step was to warm two 15ml conical tubes of Locke's solution⁴². One tube was the wash and needed 475 μ l of Locke's per well. The other tube was labeled "loading solution" (6ml for 8 wells), and had 600 μ l per well. The loading process typically took 1hr. in a 37°C incubator or 15 minutes in a 37°C water bath. Once the loading tube was warmed in sterile conditions, 5 μ l of Pluronic acid⁴³ was added, and

vortexed looking for minor bubbles to signify thorough mixing. Then, with low light conditions, 6 μ l of Flo 4AM⁴⁴ was added and vortexed. Once the solution was prepared, a plate was obtained and all media was gently removed so as not to disturb the cells⁴⁵. Next, 600 μ l of loading solution was added to the wells slowly so as not to lift the cells or unduly stress them. This was repeated on all wells. Once all wells had their media exchanged for loading solution, the cells were returned back to the incubator for 1hr.

In the meantime, all stimulants, such as ATP, experimentals, or Ionomycin were prepared. Also in this time, the imaging systems equipment, if needed, began warming up. When the 1hr. wait was up, the plate was retrieved and once again the solution was gently removed, adding the 475 μ l of plain Locke's, also known as the recovery solution, and placed back in the incubator for 20 min to reduce stress. After the 20 min had expired, the plate was ready for calcium imaging (pictured in the next page, Fig. 2-9-1).

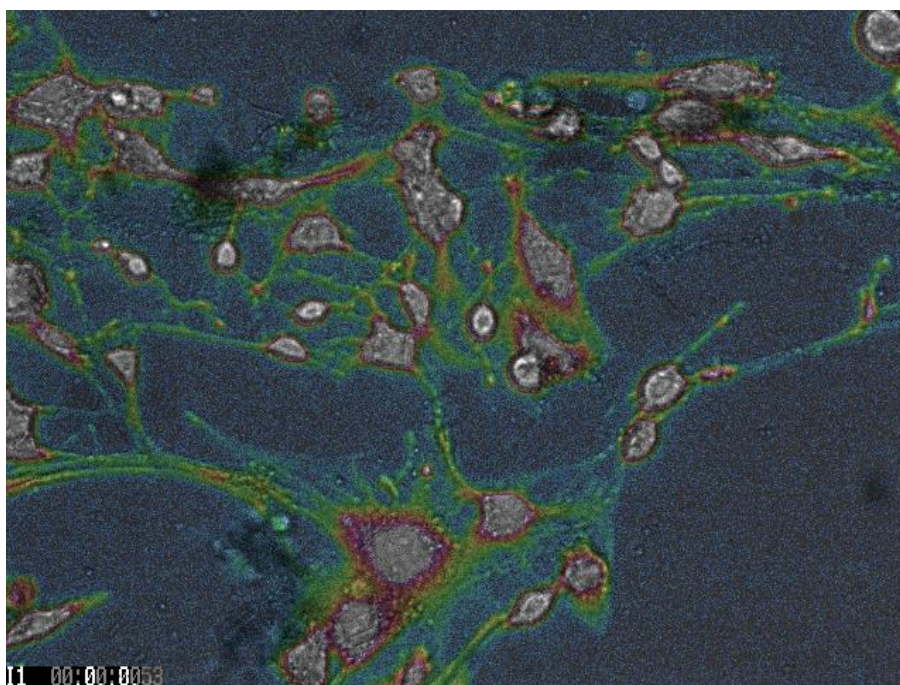


Figure 2-9-1: Above a phase light image from a calcium imaging session merged with a pseudo color image of the same frame to indicate intensity of response. This frame was taken after the addition of Ionomycin, a positive control showing maximum response.

2.10 DAPI Staining

DAPI is a technique that utilizes the fluorescent properties of the DAPI molecule^{46, 47} which selectively dyes the DNA of a cell, highlighting the nucleus and allowing imaging⁴⁸. Once a plate has been fixed for DAPI imaging, it will need the addition of DAPI diluted in sterile water. A 1:300-fold dilution was used to see successful staining of the nucleus. Exposure was set to 400ms with a gain of 3-fold in the “Ai4” setting. The purpose of DAPI staining was to highlight the morphology of the nucleus for imaging. By means of fluorescence, one can drastically increase the contrast between background noise^{49, 50} and then observe changes in roundness and area, aided by computer software. A drastic change in these values can indicate stress or abnormal growth. An example of this would be a decreased value in roundness. Shown in Figure 2-10-1 on the next page, a

flat adherent cell with processes will have a much more flattened nucleus⁵¹, and a higher roundness value as compared to a near floating cell which will have a value close to 1.

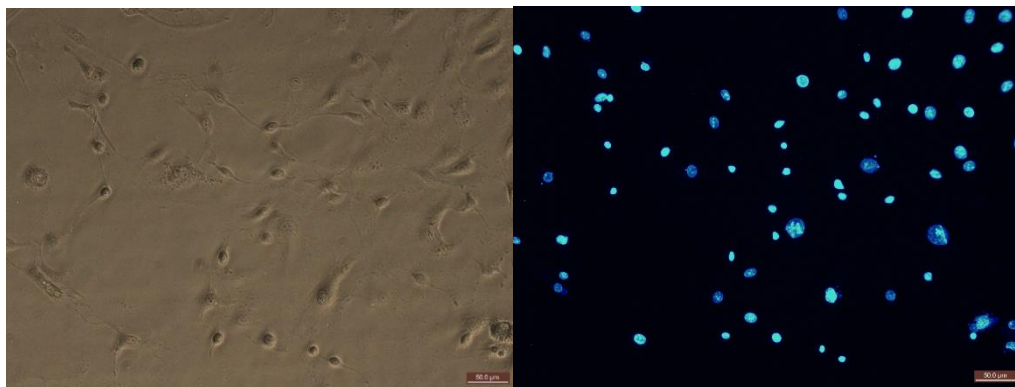


Figure 2-10-1: Above (left) glioma cells grown 5 DIV and (right) a DAPI stain of the same view. Note in the phase light image the variety of cell sizes and elongated transparent nature of the cell body and processes indicating healthy adhesion to the flask. Cells also lack a “halo” effect that may come from a cell becoming round as it lifts off the surface causing light to bend.

2.11 Image Analysis and Data Normalization

For the series of images generated from calcium imaging along with results from DAPI images, analysis and data normalization would need to be performed. In the case of calcium imaging, data processing was performed on the same system that the images were taken or a similar system with the same operating system and software version. We began by bringing up the last image(s) in each wells’s recording. This was done in all cases and the final stimuli was ionomycin 500nM; and, therefore, are the brightest calcium signaling. Once on this frame we digitally circle an Area Of Interest (AOI) to record the readings of a cell. It is important to keep the circle tight to the cell body, as including excess background will increase noise and decrease reading accuracy, dropping the overall value of intensity recorded over time. Once all AOIs in the frame have been highlighted, the location and size were saved as an “.OBJ” file. The AOIs were then copied to all frames in the session. Once this is done, we went through several various

frames to ensure we did not have a floating cell obscuring values. A measurement at this time can then be taken and saved as a separate file. This file can then be opened in a separate window that is then copied directly into Excel. This data is simply a 2-axis table of time of the frame vs which cell body recording the intensity of light recorded as a sum of the area. I.e., one pixel at max value will have a value of ten, while a cell consisting of ten of these pixels would have a sum of one hundred. In practice it is a vast array of pixel values and often far more than ten pixels.

The data from the Excel sheet was then normalized to one at time zero for each cell. This was performed by highlighting the first row of the table and creating an equation to divide the “time=zero” value of a cell by itself, and fixing the value to this first for each cell column. Once the first row is normalized, if done correctly, all values in the first column should be equal to one. Then the highlighted region is transposed down through time.

Lastly, the cells were filtered for responders vs non responders. Responders are cells that responded to stimulus, as shown by control cells to be a value of 1.2-fold or more baseline activity. The cells also typically recover towards baseline, the trend being a negative control^{52, 53}, vs. cells that only responded to ionomycin which is a positive control⁵⁴. All cells must respond to ionomycin to be considered alive. The filter of responder was a post normalization value of 1.2-fold intensity pre-addition of ionomycin. This includes the baseline time values, as changing values pre-stimulus often indicate stress or complex behaviors; both are of interest for this study. This was done using Excel, formatting values to highlight the chart in color and hand sorting cells that responded. Once the responsive cells were sorted, an average would be generated from

all cells of the same experimental conditions and plate. These averages are graphed and displayed in Chapter 3 of this work.

For DAPI images, data analysis was performed on the same internet isolated workspace as imaging was performed. First, we loaded a hard copy of Image Pro Plus version 7.0. Next, the desired image was added to the software and the cells highlighted. This can be done with one of two common ways. Either automatically contour bright objects, in which the software would draw a link encircling objects of high luminescence and display a red outline for the operator. The alternative method is to manually select colors, in which case the operator will use an ink dropper icon to manually select all colors of interest. This method allows the user to quickly create a black and white mask of all cells. A disadvantage is that the dimmer colors cannot be selected, as it will rapidly begin to occlude random areas of the image, as the filter becomes overly sensitive.

Regardless of which method the researcher uses, the next steps remain the same. The software will undoubtedly blend, merge or join two separate cells. For this, the user will make use of the “draw a line” function to draw a line between the start and finish of cell clumps. The scale bar is often seen by the software as an AOI and must be removed with the “toggle objects on and off” function. Once all corrections and editorial decisions have been made, the user will select the measurements to display. In this study, area and roundness were chosen for their indications of cell stress via nuclear morphology. Once the measurements are displayed, “copy to clip board” is used to transfer the values to an Excel file.

Once in Excel, the averages of all cells of the same plate and conditions will be generated for cell area and roundness and these two multiplied to generate the average Nuclear Area Factor (NAF), as discovered and elaborated on by DeCoster⁵⁶.

CHAPTER 3

RESULTS

3.1 Cobalt MOBS

In the following tables, the MTT absorbance data for cobalt MOBs is displayed. Three readings were taken per well. Routine blanking occurred to ensure the instrument did not drift due to lamp heat. In the case of glioma, only 24hrs. controls were taken for comparison. Note the decrease in absorbance values (decreasing symbolizing cell stress) of the CuNPs*⁵⁶ group, a positive control known to injure or stress cells, as shown in Table 3-1-1 on the following page. The metabolism, as shown, is 43% for the CuNPs which is considered a significant drop as most cells dropping under 50% have more drastic effects than slow recovery such as, mass cell death, cell de-adhesion, or are incapable of surviving and responding to environmental factors and stimuli.

For all groups following the table in Chapter 3, there are two ways to evaluate the values relative to “time” or “controls average”. A columns value can be compared to just the controls value at a single time point such as materials average absorbance at 24hrs. compared to control at 24hrs. The other option is comparing the average of both the 24 and 48hrs. control group. As both controls grew simultaneously, the only difference in the controls was the separate time points for the addition of media to simulate the effects caused by the process of the addition of materials.

3.1.1 Cobalt's MOBs Impact on Cell Metabolism

Table 3-1-1: In the table below, we see the data for glioma cells raise 5 days *in vitro* (DIV), plated at 5k cells per ml of media and dosed with 20ug/ml cobalt MOB particles. The average values of the MOBs have been compared to the times of control to normalize different unaltered cell populations. The average values of both controls have also been merged together for a secondary comparison.

Glioma Abs. Cobalt MOB @630nm 5k/ml, 20uG/ml						
	Control 24 Hrs.	Control 48 Hrs.	CuNPs 24 Hrs.	CuNPs 48 Hrs.	Cobalt Mob 24 Hrs.	Cobalt MOB 48 Hrs.
	0.736		0.272		0.552	0.521
	0.741		0.282		0.565	0.524
	0.741		0.287		0.577	0.527
	0.678		0.332		0.699	0.517
	0.682		0.324		0.701	0.537
	0.681		0.322		0.702	0.552
					0.656	0.559
					0.661	0.571
					0.662	0.574
Average	0.710	0.710	0.303		0.642	0.542
Relative Health to Time	100%	100%	43 ± 1%*		90 ± 2%	76 ± 1%
Relative Health to Controls Average	100%	100%	43%*		90%	76%

In contrast, the “healthy, normal” astrocytes are much more fragile than the cancerous glioma as shown and supported in the following tables of MTT data; having lower astrocyte metabolism compared to glioma when exposed to stimuli such as the copper here and 24hrs. cobalt. Shown below in Table 3-1-2, note that the absorbance was taken at 570nm, and this was done to increase resolution of the readings for astrocytes.

Table 3.1.2: In the table below, we see the data for astrocyte cells raise 7 days *in vitro* (DIV), plated at 5k cells per ml of media and dosed with 20ug/ml cobalt MOB particles. The average values of the MOB's have been compared to the times of control to normalize different unaltered cell populations. The average values of both controls have also been merged together for a secondary comparison.

Astrocyte Abs. Cobalt MOB @570nm 5k/ml, 20uG/ml						
	Control 24 Hrs.	Control 48 Hrs.	CuNPs 24 Hrs.	CuNPs 48 Hrs.	Cobalt Mob 24 Hrs.	Cobalt MOB 48 Hrs.
	0.508	0.417	0.132	0.131	0.323	0.36
	0.508	0.417	0.131	0.131	0.323	0.36
	0.508	0.417	0.131	0.132	0.323	0.361
					0.442	0.334
					0.443	0.334
					0.442	0.333
					0.385	0.289
					0.386	0.29
					0.385	0.291
Average	0.508	0.417	0.131	0.131	0.414	0.328
Relative Health to Time	100%	100%	26%	31%	81 ± 2%	79 ± 1%
Relative Health to Controls Average	110%	90%	28%	28%	89%	71%

3.1.2 Cobalt MOB's Impact on Cell Morphology

On the next page are DAPI staining images for glioma that were exposed to cobalt MOB's. Of note are the larger cell nuclei often present, on the next page in Figure 3-1-1. After these images, tables display the average values of area, roundness and NAF of the conditional groups from which these images were taken, Table 3-1-3.

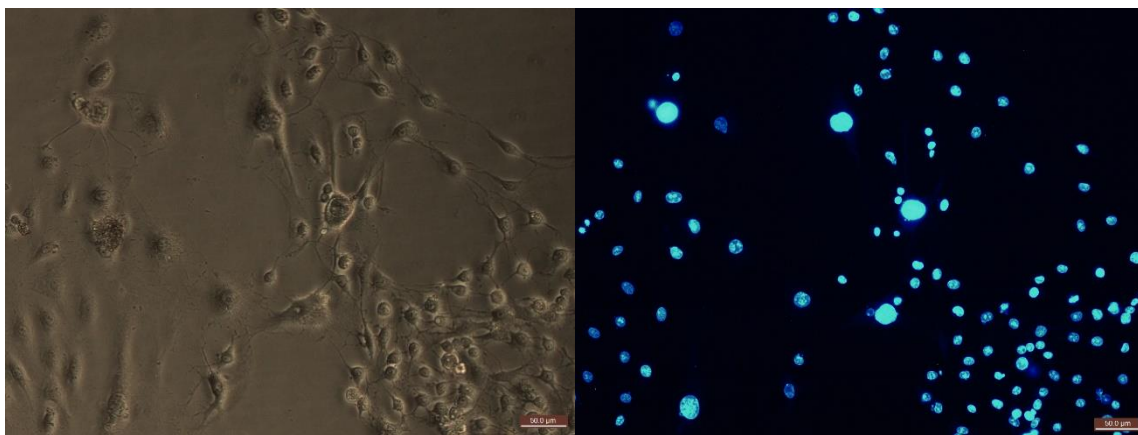


Figure 3-1-1: The above images (left) a phase light image of Cobalt MOBs 48hrs. exposure and (right) was a DAPI stain of glioma cells grown 5 DIV fixed and then stained to image. Note the larger than normal nuclei that in some Co MOB cultures were present. Scale bar 50 μ m.

Below in Table 3-1-3, we see a decrease in the cobalt roundness values compared to the controls.

Table 3-1-3: This is the DAPI stain data for glioma cells.

	Area	Roundness	NAF
Average for Controls (Co)	426.6166	1.308684	558.3064
Average for Co 24hrs	421.2918	1.268579	534.442
Average for Co 48hrs	448.0405	1.249056	559.6279

Below we see in Figure 3-1-2 two images for astrocytes exposed to cobalt MOB for 48Hrs. These cells had a similar trend of being larger than their control counterparts. Also note the presence of the Co MOB particles.

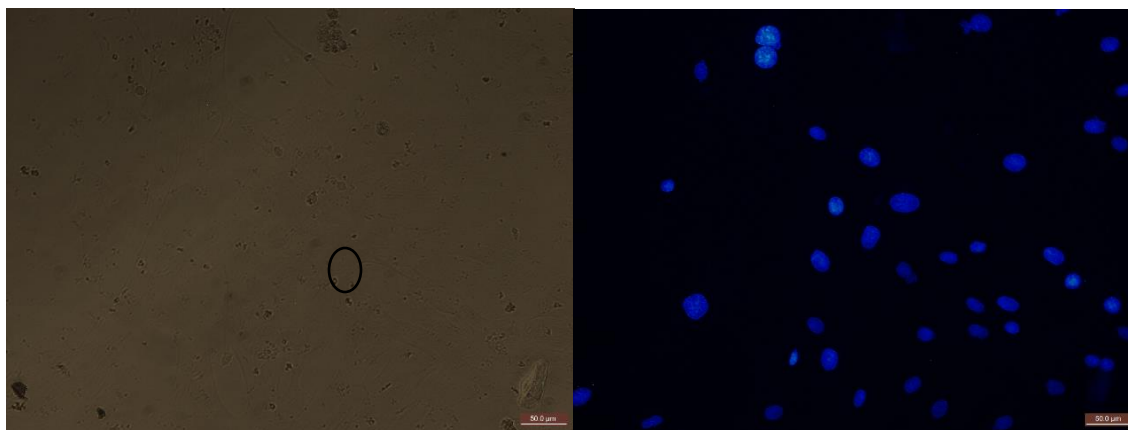


Figure 3-1-2: The above images (left) aphase light image of Cobalt MOB 48hrs. exposure and (right) was a DAPI stain of astrocyte cells grown 5 DIV fixed and then stained to image. Note the larger than normal nucleus that in some Co MOB cultures were present. This feature was also present in the astrocytes and can be shown in table 3.1.4. Scale bar = 50µm.

Below in Table 3-1-4 we see the DAPI nuclear stain data for astrocytes. Note the higher average NAF and area for both cobalt groups.

Table 3-1-4: This is the DAPI stain data for astrocyte cells.

	Area	Roundness	NAF
Average For Control	1251.917	1.2750953	1596.313
Average For Cobalt 24hrs	1443.374	1.21280342	1750.529
Average For Cobalt 48hrs	1289.618	1.2670243	1633.977

3.1.3 Cobalt MOBs Impact on Cell Response

Below is a graph of the calcium imaging data representing the cobalt MOB-exposed glioma cells and their dynamic calcium response to Ionomycin, Figure 3-1-3. Red arrows indicate the time points at which stimuli were added. In this case, stimuli were ATP 1 μ M and Ionomycin 250nM.

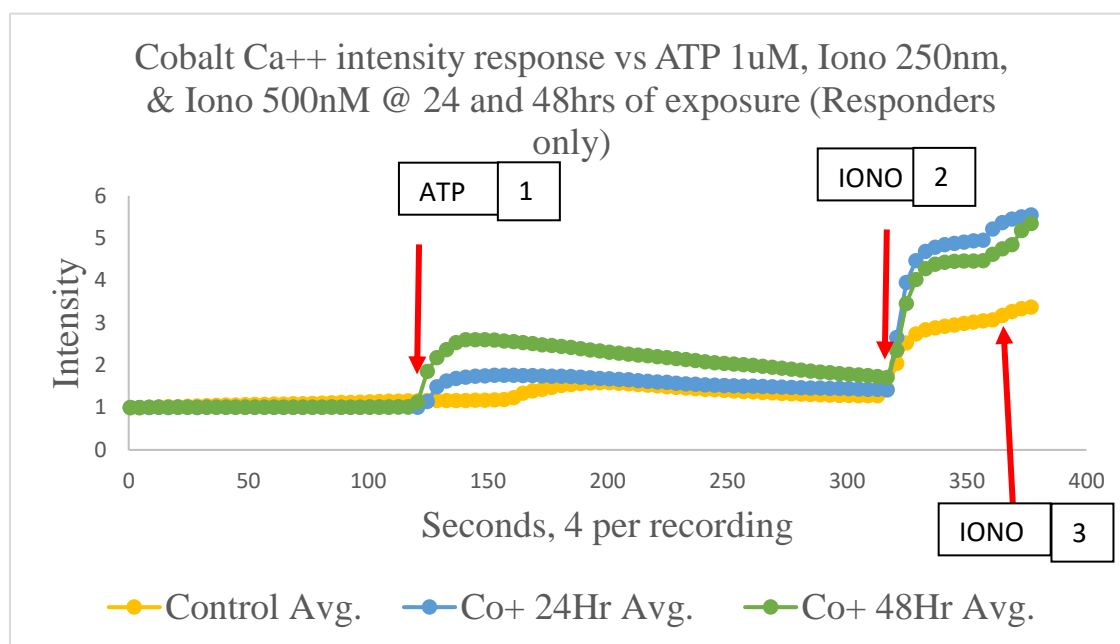


Figure 3-1-3: Calcium response data for glioma cells exposed to cobalt MOB 24 and 48 hrs. compared with a control well with no additions.

3.2 CuHARS

3.2.1 CuHARS MOBs Impact on Cell Metabolism

In the following tables, the MTT absorbance data for CuHARS is displayed. Three readings were taken per well. The relative health of the glioma versus the astrocytes is noteworthy; Table 3-2-1/2 on the next pages. A mechanism that selectively reduces the metabolism of glioma and has no, nominal, or manageable effects on astrocytes would be considered a successful treatment for cancerous tissues at this scale.

Table 3-2-1: In the table below, we see the data for glioma cells raise 5 days (DIV), plated at 5k cells per ml of media and dosed with 20ug/ml CuHARS particles. The average values of the MOBs have been compared to the times of control to normalize different unaltered cell populations. The average values of both controls have also been merged together for a secondary comparison.

Glioma Abs. CuHARS MOB @630nm 5k/ml, 20uG/ml						
	Control 24 Hrs.	Control 48 Hrs.	CuNPs 24 Hrs.	CuNPs 48 Hrs.	CuHARS 24 Hrs.	CuHARS 48 Hrs.
	0.798	0.693	0.419	0.289	0.641	0.597
	0.803	0.701	0.423	0.294	0.657	0.601
	0.807	0.709	0.425	0.3	0.668	0.607
					0.444	0.444
					0.447	0.446
					0.451	0.446
					0.609	0.539
					0.612	0.55
					0.615	0.55
Average	0.803	0.701	0.422	0.294	0.572	0.531
Relative Health to Time	100%	100%	53%*	42%*	71 ± 3%	76 ± 2%
Relative Health to Controls Average	107%	93%	56%	39%	76%	71%

Below in Table 3-2-2, keeping in mind that the values for CuHARs were $71 \pm 3\%$, $76 \pm 2\%$, note the higher values that are highlighted representing absorbance for astrocytes.

Table 3-2-2: In the table below, we see the data for astrocyte cells raise 7 (DIV), plated at 5k cells per ml of media and dosed with 20ug/ml CuHARs particles. The average values of the MOBs have been compared to the times of control to normalize different unaltered cell populations. The average values of both controls have also been merged together for a secondary comparison.

Astrocyte Abs. CuHARs MOB @570nm 5k/ml, 20uG/ml						
	Control 24 Hrs.	Control 48 Hrs.	CuNPs 24 Hrs.	CuNPs 48 Hrs.	CuHARs 24 Hrs.	CuHARs 48 Hrs.
	0.455	0.429	0.326	0.172	0.393	0.394
	0.455	0.43	0.326	0.172	0.395	0.395
	0.458	0.437	0.328	0.175	0.397	0.398
					0.327	0.233
					0.327	0.235
					0.33	0.235
					0.374	0.42
					0.375	0.422
					0.378	0.423
Average	0.456	0.432	0.327	0.173	0.366	0.351
Relative Health to Time	100%	100%	72%	40%	80 ± 1%	81 ± 3%
Relative Health to Controls Average	103%	97%	74%	39%	82%	79%

3.2.2 CuHARS MOBs Impact on Cell Morphology

Below are in Fig. 3-2-1, are DAPI staining images for glioma that were exposed to CuHARS. Of note is the clear presence of CuHARS structures, as shown by fine black lines in the phase light imagery. After these images, tables display the average values of area, roundness and NAF of the conditional groups from which these images were taken.

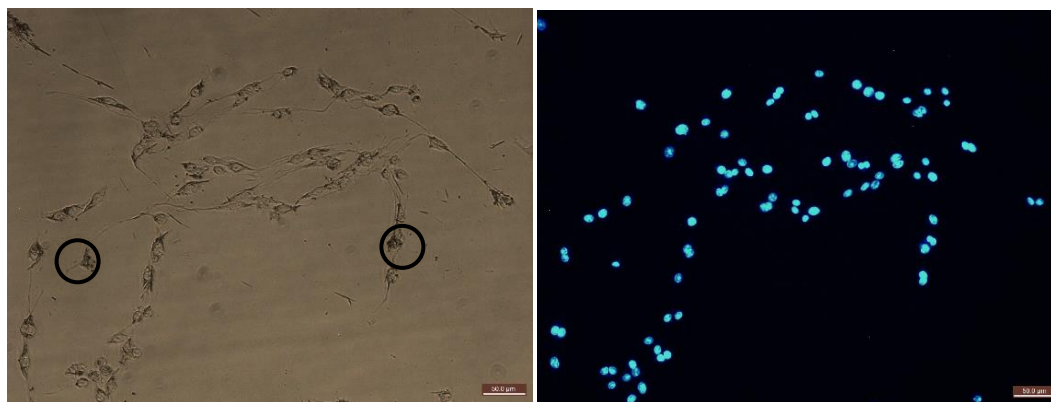


Figure 3-2-1: The above images (left) a phase light image of CuHARS 48hrs. exposure and (right) was a DAPI stain of glioma cells grown 5 DIV fixed and then stained to image.

Below we see the DAPI stain data of the cell nuclei in Table 3-2-3 which shows decrease of roundness in CuHARS, which could suggest less stressed cells.

Table 3-2-3: DAPI stain data for glioma cells.

	Area	Roundness	NAF
Average For Controls (CuHARS)	448.5647	1.294571	580.6989
Average For CuHARS 24Hrs	611.972	1.336157	817.6908
Average For CuHARS 48Hrs	519.1178	1.356752	704.3139

Below in Figure 3-2-2, we see images from the CuHARs 24hrs. exposure groups of astrocytes. In the left phase light image, note the presence of materials depicted as the dark black lines.

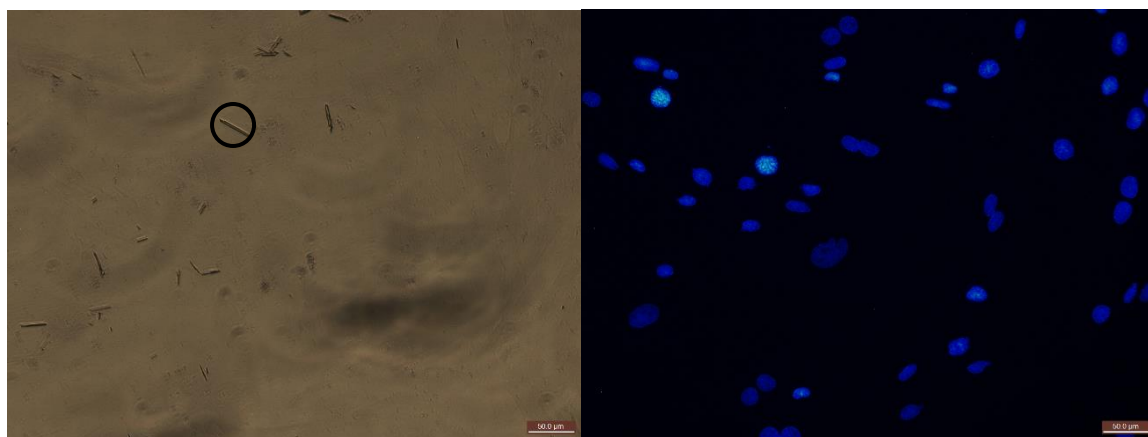


Figure 3-2-2: The above images (left) a phase light image of CuHARs 48hrs. exposure and (right) was a DAPI stain of astrocyte cells grown 5 DIV fixed and then stained to image.

Below in Table 3-2-4, we see the astrocyte DAPI staining data for CuHARs. Note the similar values of NAF for all groups and the near identical sizes for CuHARs.

Table 3-2-4: DAPI stain data for astrocyte cells.

	Area	Roundness	NAF
Average For Control	1251.917	1.2750953	1596.313
Average For CuHARs 24hrs	1206.891	1.3181766	1590.896
Average For CuHARs 48hrs	1206.452	1.35148373	1630.501

3.2.3 CuHARs Impact on Cell Response

Below is a graph representing the CuHARs exposed glioma cells calcium imaging data, Figure 3-2-3. Red arrows indicate the time points at which stimuli were added. In this case stimuli #1/2 were ATP $1\mu\text{M}$, and #3 Ionomycin 250nM . Note the peaks of stress.

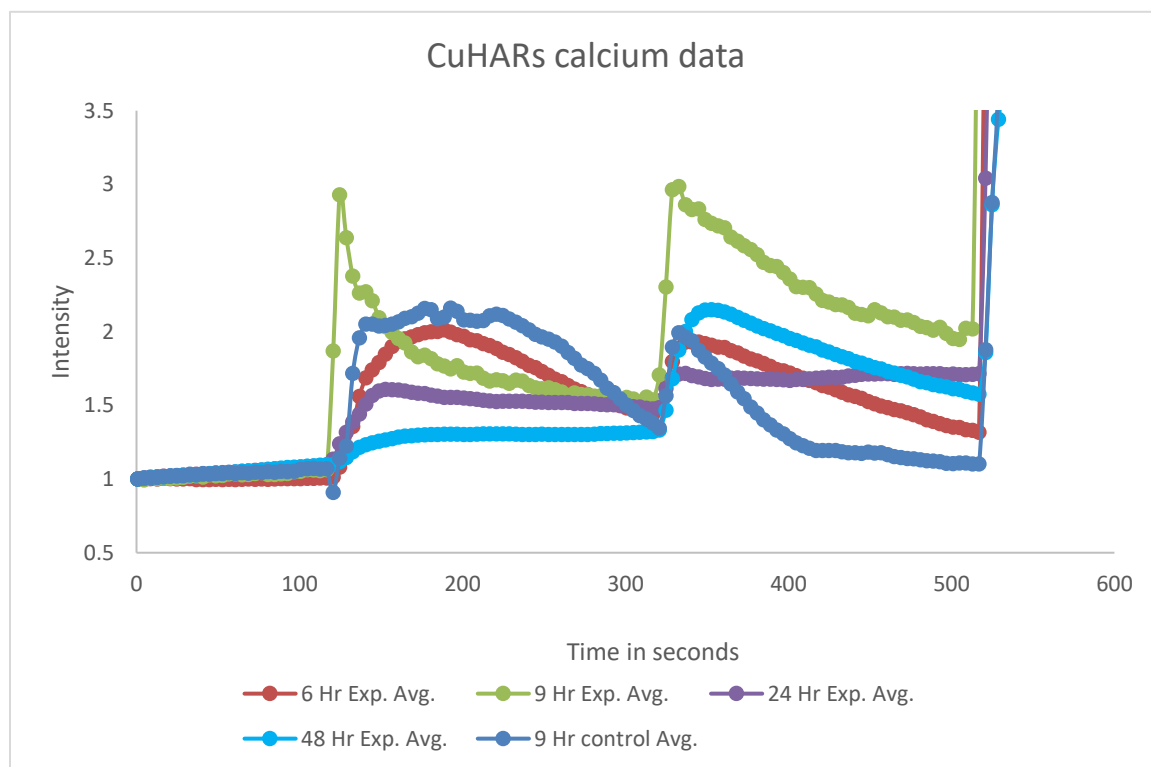


Figure 3-2-3: In the figure above, we see the calcium response data for glioma cells exposed to CuHARs MOBs 24 and 48 hrs. compared with a control well with no additions.

3.3 Zinc MOBs

3.3.1 Zinc MOBs Impact on Cell Metabolism

In the following tables, the MTT absorbance data for zinc MOBs is displayed. Of interest is the increase on initial metabolism of zinc-exposed glioma cells in the 24hrs. group. While several MOBs cause a higher 48hrs. group value than the 24hrs. group and vice versa, there has not been another MOB material showing increase in absorbance to this extent**.

Table 3-3-1: In the table below, we see the data for glioma cells raise 5 (DIV), plated at 5k cells per ml of media and dosed with 20ug/ml Zinc MOB particles. The average values of the MOBs have been compared to the times of control to normalize different unaltered cell populations. The average values of both controls have also been merged together for a secondary comparison.

Glioma Abs. Zinc MOB @630nm 5k/ml, 20uG/ml						
	Control 24 Hrs.	Control 48 Hrs.	CuNPs 24 Hrs.	CuNPs 48 Hrs.	Zinc 24 Hrs.	Zinc 48 Hrs.
	0.464	0.454	0.271	0.184	0.761	0.383
	0.467	0.456	0.272	0.185	0.769	0.387
	0.468	0.458	0.272	0.186	0.79	0.389
					0.502	0.334
					0.503	0.337
					0.505	0.342
					0.631	0.539
					0.658	0.547
					0.667	0.555
Average	0.466	0.456	0.272	0.185	0.643	0.424
Relative Health to Time	100%	100%	58%	41%	138 ± 4%**	93 ± 3%
Relative Health to Controls Average	101%	99%	59%	40%	139%	92%

Below in Table 3-3-2 we see the lowest recorded CuNPs values. Also of slight obscurities is the value for the averaged controls compared to the Zn 48hrs. in the most bottom left cell, which suggest the 48 hrs. astrocytes out-performed the glioma by 3%.

Table 3-3-2: In the table below, we see the data for astrocyte cells raise 7 (DIV), plated at 5k cells per ml of media and dosed with 20ug/ml Zinc MOB particles. The average values of the MOB's have been compared to the times of control to normalize different unaltered cell populations. The average values of both controls have also been merged together for a secondary comparison.

Astrocyte Abs. Zinc MOB @570nm 5k/ml, 20uG/ml						
	Control 24 Hrs.	Control 48 Hrs.	CuNPs 24 Hrs.	CuNPs 48 Hrs.	Zinc 24 Hrs.	Zinc 48 Hrs.
	0.432	0.486	0.106	0.097	0.464	0.469
	0.43	0.486	0.106	0.097	0.466	0.466
	0.431	0.485	0.106	0.098	0.471	0.463
					0.349	0.491
					0.349	0.493
					0.35	0.493
					0.252	0.356
					0.256	0.352
					0.256	0.353
Average	0.431	0.486	0.106	0.097	0.357	0.437
Relative Health to Time	100%	100%	25%	20%	83 ± 3%	90 ± 2%
Relative Health to Controls Average	94%	106%	23%	21%	78%	95%

3.3.2 Zinc MOBs Impact on Cell Morphology

Below, Fig 3-3-1, are DAPI staining images for glioma that were exposed to zinc MOBs. Of note is the variety of cell shapes, sizes, and brightness. The tables following display the average values of area, roundness, and NAF of the conditional groups.

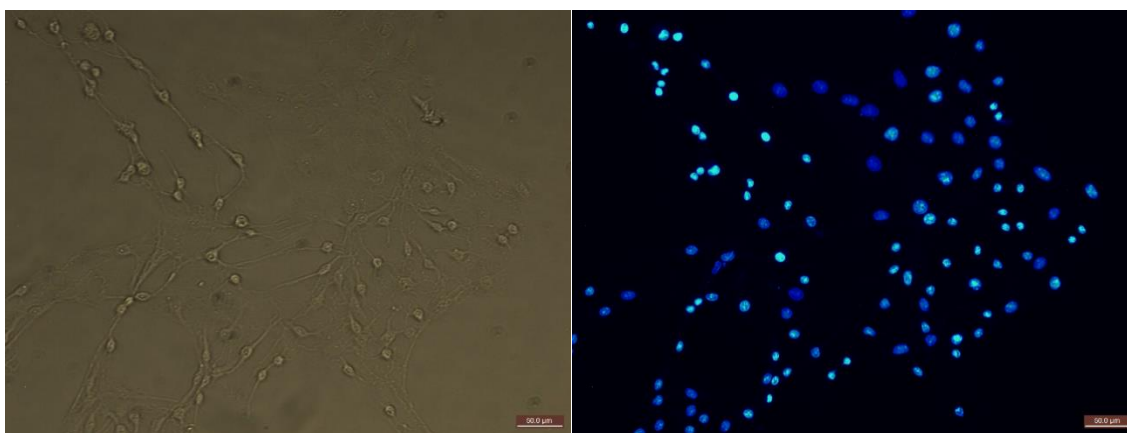


Figure 3-3-1: The above image (left) is a phase light and (right) a DAPI stain of glioma cells grown 5 DIV exposed to Zn MOBs for 48hrs. fixed and then stained to image.

In the below Table 3-3-3, we see zinc DAPI stain data for glioma. Note the similar values between both zinc groups and little change in the roundness, but a large change in area of Zn groups.

Table 3-3-3: This is the DAPI stain data for glioma cells.

	Area	Roundness	NAF
Average for Controls (Zn)	511.996	1.199097	613.8968
Average for Zn 24hrs	464.4684	1.198775	556.7929
Average for Zn 48hrs	459.3157	1.189434	546.3257

Below in Figure 3-3-2, we see a DAPI stain of astrocyte cells exposed to zinc MOBs for 48hrs.

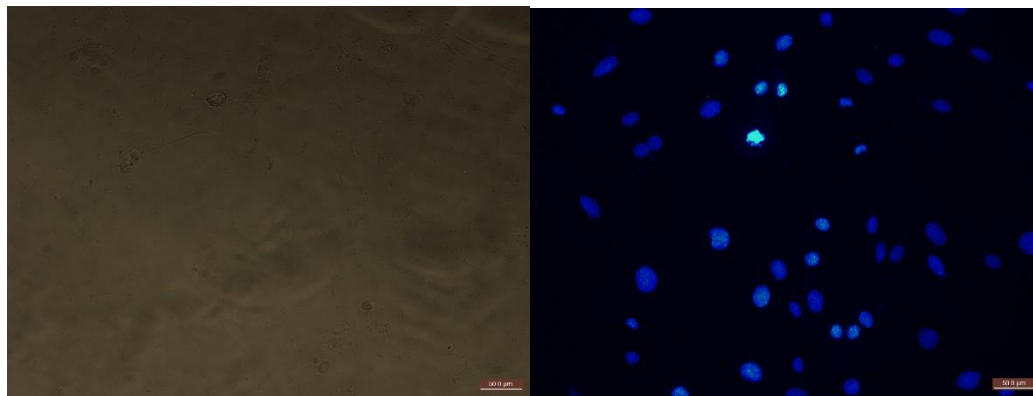


Figure 3-3-2: The above image (left) is a phase light and (right) a DAPI stain of astrocyte cells grown 5 DIV exposed to Zn MOBs for 48hrs. fixed and then stained to image.

In contrast for the astrocytes data shown below in Table 3-3-4, we see differing values between both time points for the zinc group.

Table 3-3-4: This is the DAPI stain data for astrocyte cells.

	Area	Roundness	NAF
Average For Control	1251.917	1.2750953	1596.313
Average For Zinc 24hrs	1085.653	1.38035696	1498.588
Average For Zinc 48hrs	1282.989	1.32228516	1696.478

3.3.3 Zinc MOBs Impact on Cell Response

Below in Fig. 3-3-3, is a graph representing the zinc MOBs exposed glioma cells.

Red arrows indicate the time points at which stimuli were added. In this case stimuli were #1/2 ATP 1 μ M and #3 Ionomycin 250nM.

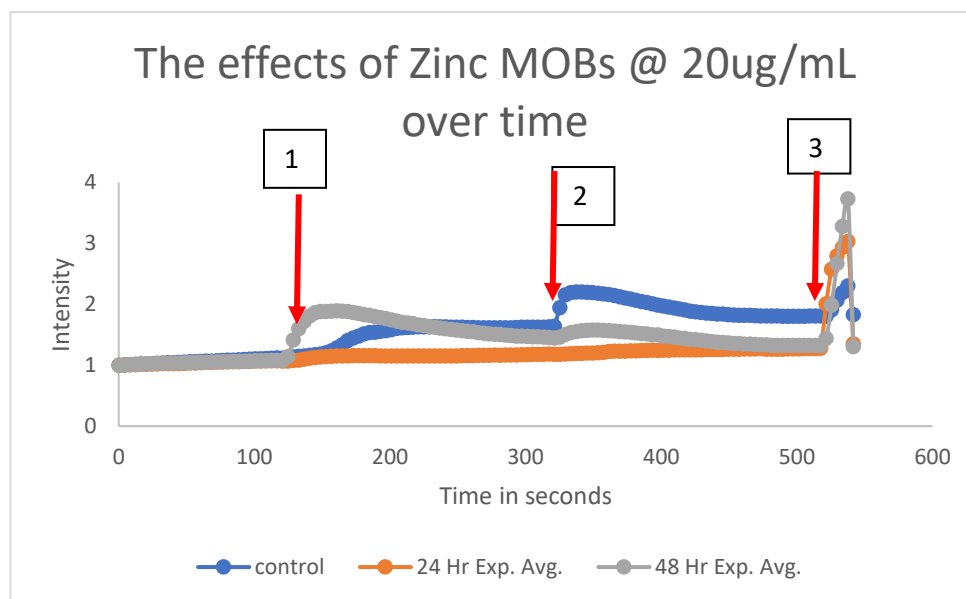


Figure 3-3-3: In the figure above, we see the calcium response data for glioma cells exposed to zinc MOBs 24 and 48 hrs. compared with a control well with no additions. Note the stress peaks in the 48hrs group and lack of response from the 24hrs group.

3.4 Silicon Dioxide NPS

3.4.1 Silicon NPS impact on Cell Metabolism

On the next page in Table 3-4-1, the MTT absorbance data for silicon dioxide nanoparticles exposed glioma is displayed. Note the similarity of values of the SiO₂ compared to that of the controls.

Table 3-4-1: In the table below, we see the data for glioma cells raise 5 (DIV), plated at 5k cells per ml of media and dosed with 20ug/ml SiO₂ particles. The average values of the MOBs have been compared to the times of control to normalize different unaltered cell populations. The average values of both controls have also been merged together for a secondary comparison.

Glioma Abs. SiO ₂ @630nm 5k/ml, 20uG/ml						
	Control 24 Hrs.	Control 48 Hrs.	CuNPs 24 Hrs.	CuNPs 48 Hrs.	SiO ₂ 24 Hrs.	SiO ₂ 48 Hrs.
	0.672	0.728	0.435	0.223	0.721	0.668
	0.679	0.73	0.44	0.236	0.725	0.674
	0.683	0.732	0.443	0.239	0.729	0.682
					0.665	0.635
					0.671	0.647
					0.679	0.658
					0.643	0.821
					0.661	0.828
					0.663	0.832
Average	0.678	0.730	0.439	0.233	0.684	0.716
Relative Health to Time	100%	100%	65%	32%	101 ± 1%	98 ± 3%
Relative Health to Controls Average	96%	104%	62%	33%	97%	102%

Once again, as shown in Table 3-4-2 on the following page, we see the astrocyte data contains similar values for the SiO₂ groups compared to the controls.

Table 3-4-2: In the table below, we see the data for glioma cells raise 7 (DIV), plated at 5k cells per ml of media and dosed with 20ug/ml SiO₂ particles. The average values of the MOB's have been compared to the times of control to normalize different unaltered cell populations. The average values of both controls have also been merged together for a secondary comparison.

Astrocyte Abs. SiO ₂ @570nm 5k/ml, 20uG/ml						
	Control 24 Hrs.	Control 48 Hrs.	CuNPs 24 Hrs.	CuNPs 48 Hrs.	SiO ₂ 24 Hrs.	SiO ₂ 48 Hrs.
	0.598	0.685	0.535	0.799	0.733	0.607
	0.603	0.688	0.539	0.804	0.731	0.608
	0.604	0.688	0.539	0.807	0.732	0.608
					0.719	0.636
					0.723	0.639
					0.725	0.64
					0.382	0.737
					0.385	0.74
					0.387	0.743
Average	0.602	0.687	0.538	0.803	0.613	0.662
Relative Health to Time	100%	100%	89%	117%	102 ± 6%	96 ± 2%
Relative Health to Controls Average	93%	107%	83%	125%	95%	103%

3.4.2 Silicon NPS Impact on Cell Morphology

Following are DAPI staining images for glioma that were exposed to SiO₂ NPS.

Of note is the cell density of Fig. 3-4-1 (SiO₂) on the following page compared to that of earlier Figure 2-10-1 (a control). After Fig. 3-4-1, tables display the average values of area, roundness and NAF of the conditional groups from which these images were taken.

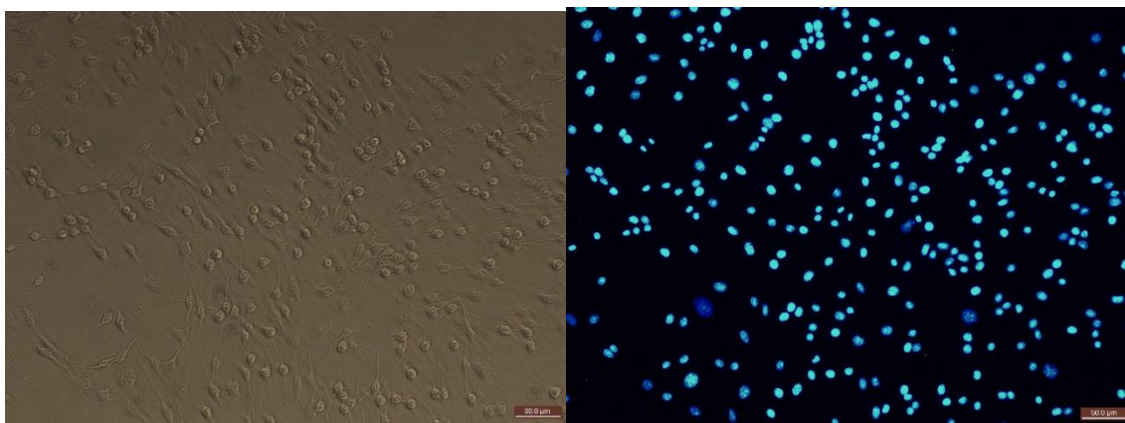


Figure 3-4-1: The above images (left) a phase light image of SiO₂ nanoparticles 24hrs. exposure and (right) was a DAPI stain of glioma cells grown 5 DIV fixed and then stained to image. Note the diversity of cell size and transparent bodies sans “halo”.

Below in Table 3-4-3, note the higher NAF and area values of the silicon groups compared to the controls.

Table 3-4-3: This is the DAPI stain data for glioma cells.

	Area	Roundness	NAF
Average for Controls (SI/np)	249.6741	1.455241	363.3361
Average for Si 24hrs	325.1977	1.298094	422.1371
Average for Si 48hrs	289.3184	1.429312	413.5264

Below in Figure 3-4-2, we see a DAPI stain and phase light image of astrocyte cells exposed to SiO₂ NPs for 48hrs. Note the variety of cells size and shape along with an observed larger size. This was the largest single group of astrocytes by area.

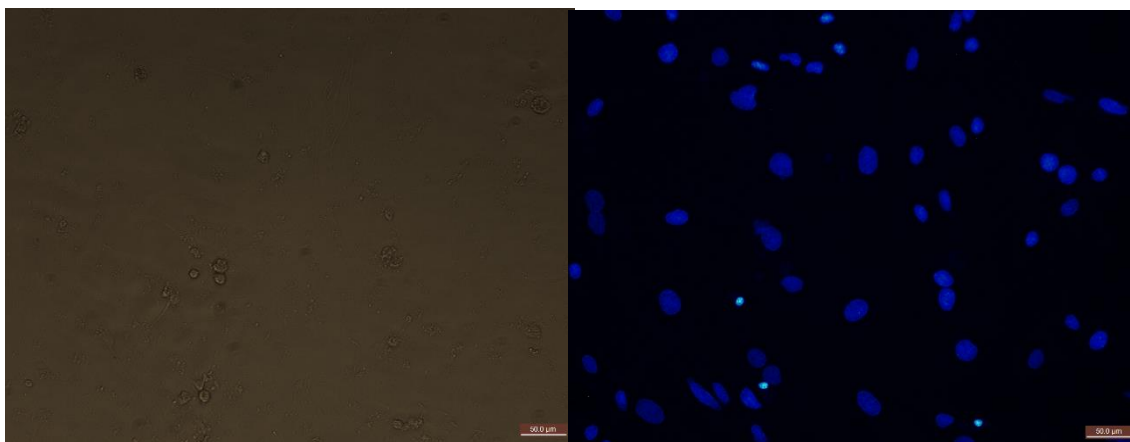


Figure 3-4-2: The above images (left) a phase light image of SiO₂ nanoparticles 24hrs. exposure and (right) was a DAPI stain of astrocyte cells grown 5 DIV fixed and then stained to image.

Below, Table 3-4-4, we see the DAPI stain values of SiO₂ NPS on astrocyte cells.

Table 3-4-4: This is the DAPI stain data for astrocyte cells.

	Area	Roundness	NAF
Average For Control	1251.917	1.2750953	1596.313
Average For SiO ₂ 24hrs	1120.047	1.29393276	1449.265
Average For SiO ₂ 48hrs	1492.218	1.25746345	1876.409

3.4.3 Silicon NPS Impact on Cell Response

On the next page, Fig. 3-4-3, is a graph representing the SiO₂ NPS-exposed glioma cells. Red arrows indicate the time points at which stimuli were added. In this case, stimuli were #1 ATP 1μM and #2/3 Ionomycin 250nM. Of note is the 1.2x baseline intensity response of the SiO₂ exposed cells. The data for only living and responsive cells are displayed. The graph has been cropped to provide resolution of the SiO₂ groups, and the controls post-ionomycin data is not displayed. Observe the third stimulus which seems to show the decrease of cell signaling from the 48hr. group, which could be an

error. However, the SiO₂ NPS are hollow and can adsorb as well as absorb, possibly up-taking some stimulus compounds. SiO₂ NPS in the 48 groups could have had a higher remaining mass of materials during the imaging session.

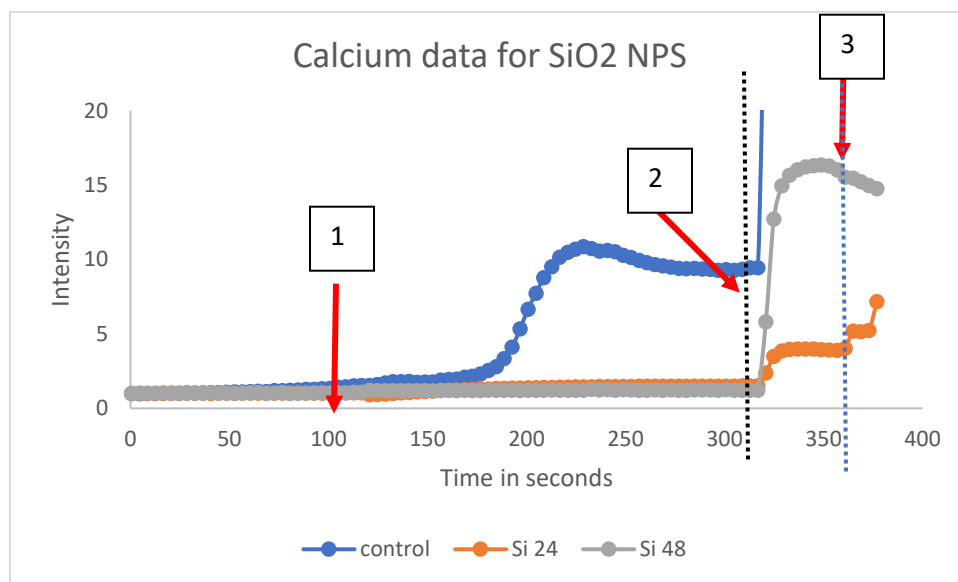


Figure 3-4-3: In the figure above, we see the calcium response data for glioma cells exposed to silicon dioxide nanoparticles 24 and 48 hrs. compared with a control well with no additions.

3.5 Copper Nanoparticles

3.5.1 The Impact of CuNPs on Cell Metabolism

On the next page in Table 3-5-1, the MTT absorbance data for CuNPs is displayed. Note the values of the CuNPs compared to the CuHARs, keeping in mind that the concentration of the CuNPs is half by mass compared to CuHARs.

Table 3-5-1: In the table below, we see the data for astrocyte cells raise 7 (DIV), plated at 5k cells per ml of media and dosed with 20ug/ml CuHARs particles. The average values of the MOBs have been compared to the times of control to normalize different unaltered cell populations. The average values of both controls have also been merged together for a secondary comparison.

Astrocyte Abs. CuHARs @570nm 5k/ml, 20uG/ml for CuHARs 10ug/ml for CuNPs						
	Control 24 Hrs	Control 48 Hrs	CuNP 24 Hrs	CuNP 48 Hrs	CuHARs 24 Hrs	CuHARs 48 Hrs
	0.624	0.302	0.539	0.644	0.56	0.479
	0.624	0.299	0.539	0.641	0.56	0.479
	0.626	0.298	0.539	0.64	0.557	0.475
	0.58	0.59	0.54	0.582	0.578	0.684
	0.582	0.589	0.538	0.578	0.576	0.684
	0.582	0.589	0.538	0.58	0.577	0.681
Average	0.603	0.445	0.539	0.611	0.568	0.580
Relative Health to Time	100 ± 1%	100 ± 6%	89 ± 0%	137 ± 1%	94 ± 0%	131 ± 5%
Relative Health to Controls Average	115%	85%	103%	117%	108%	111%

3.5.2 CuNPs Impact on Cell Morphology

On the next page, Figure 3-5-1, are DAPI staining images for glioma that were exposed to CuNPs. Note the frequency of the “halo” effect, which indicates lift due to extreme stress on cells in the phase light image. After these images, tables display the average values of area, roundness and NAF of the conditional groups from which these images were taken.

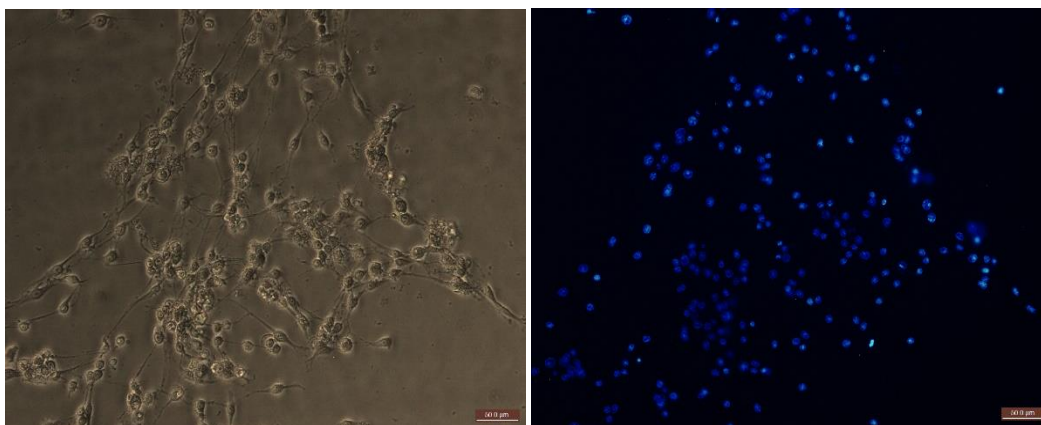


Figure 3-5-1: The above images (left) a phase light image of CuNPs 24hrs. exposure and (right) was a DAPI stain of glioma cells grown 5 DIV fixed and then stained to image. Note the smaller, round cell bodies and “Halo” effect around objects indicating lift.

Below in Table 3-5-2, we see the CuNPs data for glioma cells. Note the increase in NAF values for the CuNPs groups.

Table 3-5-2: This is the DAPI stain data for glioma cells.

	Area	Roundness	NAF
Average for Controls (SI/np)	249.6741	1.455241	363.3361
Average for CuNPs 24hrs	271.3318	1.51168	410.1669
Average for CuNPs 48hrs	311.1152	1.383619	430.4647

On the next page in Figure 3-5-2, we see a DAPI stain and phase light image of cells exposed to CuNPs for 48hrs. Note the non-discreet haze of blue as opposed to the usual oval packet. This is likely free floating nuclear material from ruptured cells. Also note the presence of materials.

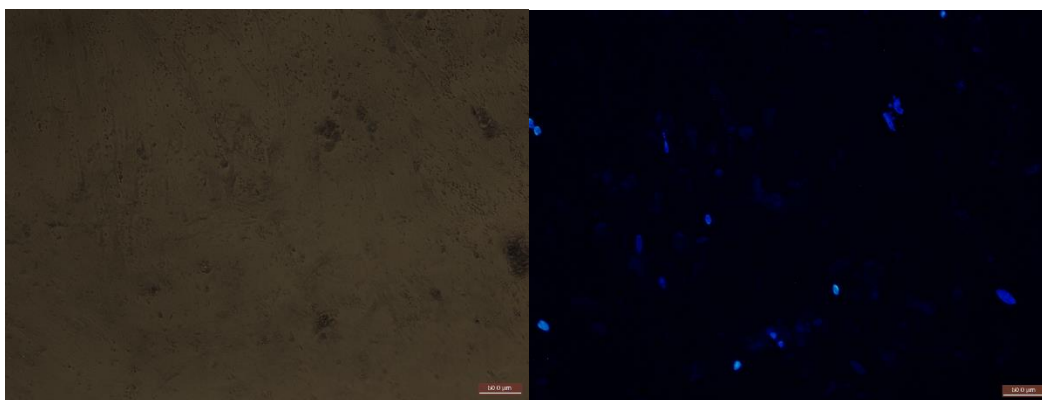


Figure 3-5-2: The above images (left) a phase light image of CuNPs 24hrs. exposure and (right) was a DAPI stain of glioma cells grown 5 DIV fixed and then stained to image. Note the none discreet haze of blue opposed to the usual oval packet. This is likely free floating nuclear material from ruptured cells.

In contrast to the glioma, the astrocytes have more of a trend in the DAPI stain data with both CuNPs groups having a large decrease in area values and lower NAF, but higher roundness values. This data is shown below in Table 3-5-3.

Table 3-5-3: This is the DAPI stain data for astrocyte cells.

	Area	Roundness	NAF
Average For Control	1251.917	1.2750953	1596.313
Average For CuNPs 24hrs	431.7826	1.38573555	598.3365
Average For CuNPs 48hrs	890.7727	1.49013525	1327.372

3.5.3 CuNPs Impact on Cell Response

Below is a graph representing the CuNPs-exposed glioma cells. Red arrows indicate the time points at which stimuli were added. In this case, stimuli were # 1 ATP 1 μ M and #2/3 Ionomycin 250nM. Of note is rapidness and intensity of the 48hrs. exposure group, indicating stress compared to that of the control and 24hrs. group in Figure 3-5-2 at the first addition.

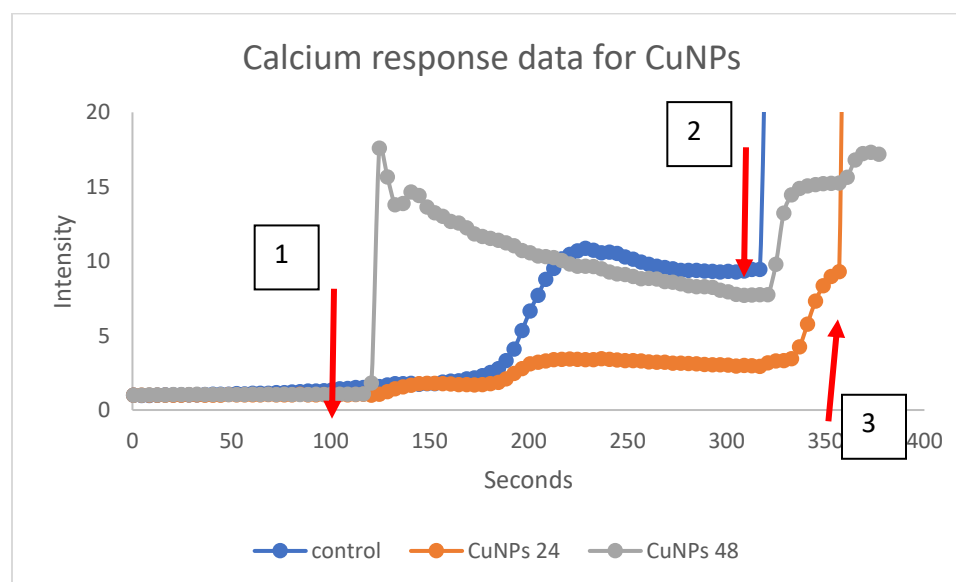


Figure 3-5-3: In the figure above, we see the calcium response data for glioma cells exposed to copper nanoparticles 24 and 48 hrs. compared with a control well with no additions. Note the rapid response of the 48hrs. group and the high intensity peak indicating stress.

CHAPTER 4

DISCUSSION

Below is Table 4-1-1, summarizing the comparative effects of each material⁵⁷

from Chapter 3.

Table 4-1-1: In the table we see a summary of major qualities of each material on cells compared to controls. The CuNPs in the table will reference them as a negative control at 20µg/ml not the 10µg/ml experiment. The format presented is follows G1,2/A3,4. 1=glioma at 24hrs, 2= glioma at 48hrs, 3= astrocytes at 24hrs and 4=astrocytes at 48hrs.

	MTT (24/48)	Calcium imaging	Observed Color	Settling	Degradability
Cobalt Mobs	G--/A--	stimulative	Yellow/Brown	++	/
CuHARs	G--/A--	stimulative	Baby blue	++	++
Zinc MOBs	G+-/A--	stimulative	White	+	+++
SiO2 NPS	+/- 2% neutral	suppressive	White	+++	----
CuNPs	EXTREMELY NEG.	Hyper stimulative/ suppressive	Grey/Ink	+++	+++

4.1 The Impact of Cobalt MOBs on Cells

As shown earlier in Table 3-1-1, the cobalt MOB had a detrimental effect on the glioma cells reducing their metabolism to 90% and 76% for 24 and 48hrs. respectively. The healthy astrocyte cells were also negatively affected, being reduced to 89% then 71% as shown in Table 3-1-2. This impact on the astrocytes suggests that, with time, the cancerous glioma may be able to better cope with the cobalt MOB treatment.

In Figure 3-1-3, we see the calcium imaging data for cobalt on glioma. When comparing the response to ATP 1 μ M, the longer the cells were exposed to MOBs, the greater the intensity of response from the cells. At 48 hours the intensity of response was ~2.25 fold greater. The higher the intensity of response, the more likely a cell is to be stressed. At 250nm of ionomycin, the 24hrs. response takes over as the most prominent followed shortly by the 48hrs. and finally 2/3 the intensity of response was the control group. Subsequent 500nm of ionomycin showed similar minor increases of response from all groups.

The DAPI stains revealed some interesting morphologies of cobalt MOB exposed glioma cells. The most stand-out characteristic observed was the presence of much larger than normal cells. At first, I believed this to be a field-of-view issue catching outliers. However, in every well while not prevalent and predominant, the enlarged Co-exposed cells were significantly present. This was the condition that most fell in line with the initial hypothesis of the effects of MOBs; minor stress, an array of healthy and stressed morphologies. The “halo” effect is present on some cells but not all. In fact, when looking between the left and right of the presented image for cobalt MOBs in phase light (Figure 3-1-2), it’s almost a tale of two cities. On the left, it is hard to separate from the

background because the cells are so well adhered; on the right shows the beginning signs of significant stress. The astrocytes also shared the trend of increased cell size visually, Table 3-1-4, and numerically displayed this in area and NAF. While in roundness both were lower than control, suggesting possible osmotic swelling which would also explain increase in area.

4.2 The Impact of CuHARs on Cells

Most fascinating was the MTT metabolism data from CuHARs. The metabolism of astrocytes out performed that of the glioma by a minimum of 5%, Table 3-2-1/3-2-2. This suggest that the copper-based MOB is possibly capable of undermining the stability of glioma control over a multicell-type environment.

These results were then cross examined with a second MTT test comparing the standard dosage 20 μ g/ml of CuHARs vs. only 10ug/ml of CuNPs. This was done not only to increase the data pool on this subject, but also to support the claim that MOBs are less harsh than their regular nanoparticle counterparts.

The secondary reason for this is that the exact composition of both is unknown; that is to say that while both have copper, not all 20 μ g/ml is copper. With rough approximations of each materials' copper content, see Figure 2-2-(1-5), by halving the amount of CuNPs it is fairly certain the CuHARs would have less free copper ions at any moment and similar amounts of copper by mass. The effects would then be further isolated to the CuHARs having a slowed reaction kinetic due to reduced surface area per mass. For example, assuming all CuNPs are CuO₂, the least copper bearing form, any mass would be 66.51% copper. Opposite is CuHARs in which the most copper bearing of the proposed structures would be 34.41% copper mass. Now, these numbers applied to

the 20 μ g/ml of CuHARs vs. only 10 μ g/ml of CuNPs would put the mass of copper present at similar levels, slightly more in the CuHARs. The data seems to agree with this in Table 3-5-1, showing they are similar in relative MTT health.

However, this is when the chemistry is most in favor to disprove the hypothesis that raw nanoparticles are less impactful on cell health than a MOB counterpart. In reality the CuNPs used were an unknown mixture of CuO and CuO₂, and the CuHARs were likely a mix of all three proposed structures that can contain possibly unreacted cysteine or have other unknown hydrocarbon R-groups.

The CuHARs were being examined with calcium imaging much earlier in the course of my research at a level of detail that would not be continued, as it did not allow time to investigate other materials or cell lines at acceptable levels. That said, the level of insight on these groups is particularly fascinating in regards to glioma calcium imaging with not two time points, but four. The trend we see in Figure 3-2-2 at the first 1 μ M ATP stimulus through time exposed to CuHARS is that the cells have an initial suppression followed by agitation, and then progressively lower response, more so than the six hours' group (200/220 total cells responding). The second 1 μ M ATP response is similar in regards to the six- and nine-hour time points (63/66 total cells responding), but at 24 hours, the group (156/166 total cell responding) never had a significant recovery and just raised the plateau of agitation. Meanwhile the 48 hours' group (116/132 total cells responding) went from a low response, to the first stimulus, to having a greater intensity than the control group.

When observing the DAPI data in Table 3-2-3, the glioma had increased values in all regards compared to controls. This suggests a possible slight stunting in early

development followed by a recovery. The astrocytes in Table 3-2-4 have an extremely consistent value for area and higher degrees of roundness when compared to controls. In comparison to control in all fields, they are fairly similar.

4.3 The Impact of Zinc MOBs on Cells

Zinc is prevalent in the body, used in our zinc finger proteins for critical roles in DNA and RNA handling along with transcription⁵⁸. It is also the second most common trace metal, only bested by iron. Lack of zinc can also cause anemia, fainting, dietary uptake issues, and nervous system failures⁵⁹.

Zinc MOBs exposed glioma had an unusual reaction, with an initial spike in metabolism at 24hrs. to 139% (Table 3-3-1) then dropping to 92% at 48hrs. While this trend may seem to be the source of under/overdosing, it is not too dissimilar from conditions such as fever where metabolism is raised to fight adverse conditions. However, just as with fevers, this state is not sustainable and then collapses to a lower rate. Also, of slight curiosity is the astrocytes (Table 3-3-2) which dropped to 78% but seemingly recovered to 95%; above the glioma by 3%.

In terms of glioma calcium response, the 24hrs. group was suspected to be dead; but, ionomycin and review of the calcium video data suggests that the cells are heavily suppressed, as there are only minor responses. While poorly understood, we know Zn is capable of suppressing certain protein expressions and transcriptions of RNA⁶⁰. Countering this is the trend at 48hrs., showing a very immediate response to the first stimulant compared to most glioma controls; almost like a hair trigger. While the intensity of the response did not exceed that of the control groups, this behavior is

abnormal. The secondary stimulus also shows a minor reaction, showing the cells were still capable of resisting the effects of ionomycin as a healthy cell sometimes can.

When observing the DAPI data for the glioma cells in Table 3-3-3, it seems to have negatively impacted the glioma in all categories; most significantly in many cells' area. When turning our attention to Table 3-3-4 for the astrocyte data, we see a more exciting trend for the initial astrocytes in the 24 hrs. Zn MOBs group. These do not perform as well in all categories, but seem to improve by the 48hrs. group surpassing the controls, possibly suggesting recovery. In this stand-out observation, Zn MOBs seem to also be capable of selectively targeting glioma over astrocytes

4.4 The Impact of Silicon Dioxide Nanoparticles on Cells

The silicon dioxide, Tables 3-4-1/3-4-2, showed an expected low deviation of results (max standard deviation of the mean being 5% between cell types). All results for the experiments hovered around 100%, supporting the neutrality of SiO₂.

The DAPI stains of glioma also seemed to confirm this, having a vast array of cell types, sizes and good adhesion visually, Fig 3-4-1. Numerically in Table 3-4-3, we see the data for glioma DAPI stains which suggest the glioma are out-performing the controls in area and NAF. The astrocytes in Table 3-4-4 at 24hrs. are negatively impacted compared to controls and at 48hrs. which are positively impacted.

In direct conflict were the results on the glioma from calcium imaging sessions, which showed that it entirely suppressed a response from the SiO₂ groups. While they did respond to ionomycin, indicating their viability as a sample, it was significantly reduced compared to that of the control group. These results combined could suggest that SiO₂ nanoparticles can insulate cells from rapid changes in the environment. While the 24hrs.

group did continue to increasingly respond to the ionomycin until the end of the recording session, the 48hrs. group did not. The SiO₂ NPS used here are hollow and can adsorb as well as absorb, and possibly could be taking up some stimuli molecules. Also, the better incorporated SiO₂ NPS could have had a higher remaining mass during the imaging session.

4.5 The Impact of Copper Nanoparticles on Cells

As an industry control, the CuNPs effects should be evaluated as a comparison for other materials effects. As show in most tables in Chapter 3, CuNPs significantly reduced the metabolism of both cells. When averaged by health across all experiments, the 24hr. exposure reduced by 54% in glioma and 53% in astrocytes. Similarly, for the 48hr. group, glioma dropped to 38% and astrocytes to 31%. These effects were consistent with the literature⁵⁶.

Glioma DAPI data, Table 3-5-2 on the CuNPs revealed extremely damaged morphologies. Typically, broad, flat blades of cell processes had become spindly spider webs. Once, hard-to-distinguish nuclei became swollen beads on a string of detaching extremities. The “halo” of light suggests the near release of all cells present. Mind that all DAPI stains are done after fixation and a wash, meaning the “worst” cells are already removed. These are simply the next group whose average was just good enough to stick and be used. Of the cells present in this observation, 436 were in the 48hrs. group, 430 cells in the 24hrs group, and 2,522 cells in the control group of this plate.

The astrocytes showed extreme damage as well in Figure 3-5-3. It can be seen that the once discreet star like regions of cells have now gone super nova (ruptured) into loose nebulas; their nuclear material scattered into the surrounding area.

CHAPTER 5

CONCLUSIONS AND FUTURE WORKS

5.1 Conclusions

In regards to the earlier hypothesis made on cells, SiO₂ had a minimal impact on the cells health only having a deviation +/- 3% of relative normal metabolism (Figure 3-4-1/2). This was also on display in the DAPI and phase light imaging with a fairly dense and varying adherent morphologies of cells observed (Figure 3-4-1). However, the calcium imaging data available (Figure 3-4-2) suggests it may be capable of suppressing immediate response to the environment; this being counter to what was expected and known of other brain cells⁶¹.

Cobalt MOBs in all tests showed signs of stress, and while the calcium imaging data may suggest mild long-term suppression, when combined with the MTT results it is suggested that astrocytes are more heavily suppressed. Also, the DAPI data in accord I would not recommend it at the current 20µg/ml dosage to be further studied or utilized, as the effects were too harsh. This supports the earlier hypothesis that Co MOBS would be harsher than CuHARs, but less harsh than CuNPs.

The zinc was capable of showing 24hr. group suppression followed by signs of recovery at 48hrs. in the calcium imaging data and, coupled with the MTT data, this seems possible. However, the key factor for my recommendation of further study is the

DAPI data. When comparing the two, the astrocytes seem to have had a less negative response when compared to the glioma from examining roundness in Table 3-3-4.

The apparent stars of the show were the optimal CuHARs effects, decreasing metabolism of glioma to 76% efficiency at 24 hrs. and 71% at 48 hrs., while leaving the astrocytes at 82% and 79% respectively (Table 3-2-1/2). The data from the later test of CuNPs 10 μ g/ml vs. the CuHARs remaining at 20 μ g/ml (Table 3-5-3) is somewhat inconclusive-to slightly supportive of the earlier hypothesis of MOB's having a less harsh effect on cell health compared to a raw nanoparticle counterpart (Table 3-5-1). Both compounds had similar effects on the cell's metabolism, but the mass of copper was higher in CuHARs and performed better at the 24hrs. mark and worse at the 48hrs. mark. This could indicate a slower release of copper ions into the environment. The data collected on CuNPs only served to compound the common understanding of their toxic effects on cell health.

Speaking to metabolism results where the controls were at 100%, while a material may be at 130% at 48hrs., a likely conclusion may be made: population control. If, per say, a culture has to last 5 days at full-function uninhibited, but only has 3 days of resources, it would not survive. However, if one were to slow the metabolism it may last, as the cells were not capable of growing at the same rate. If both conditions were examined at day 4, the delayed reduction in metabolism of cells would appear to have outperformed the control. In the same sense, the controls may have been reaching a state of exhaustive resources; not acidic enough or low enough on nutrients to kill but to diminish growth. Meanwhile, the cells that have just finished processing a material (Fig 3-5-1) are on the up-and-coming.

5.2 Future Works

Carrying this work forward, I would like to investigate the reactions of a co-culture of glioma and astrocyte cells⁶². The diseased brain is never truly only “healthy” or diseased. By attempting to model a more holistic view of a typical cancer patient of each cell type, by plating at a similar cell density as in a patient, we may gain better understanding of the response of materials *in vivo*.

Seeing the work that is comparing the CuNPs at varying dosages (3.5), it begs the question of what concentrations are any of the MOB/NPS effective; as it may be but a slight factor needed to turn the tide against glioma. Perhaps even lowering the dosage of a successful treatment but periodically dosing a co-culture could selectively deplete it of cancerous cells. X-ray diffraction (XRD) could be used to determine the metal by mass of each of the compounds.

Next, there were several other MOB that time did not permit the study of such as gold, silver and iron. All of which have shown similar promise in regards to internal medicine and related work^{6, 7}.

Nitric oxide assay⁶³ would be one of the many additional ways I would like to evaluate cell culture stress. Release of NO by endothelial cells is shown to relax blood vessels and increase blood flow. By examining the release of this gas⁶⁴, we may be able to determine if the cells are signaling inadvertently for more or less oxygen among other blood delivered resources, which could indicate stress.

Another assay I would like to perform is referred to as Diff-Quik. This assay is useful for its multicolored staining of cellular components, allowing evaluation of the nuclear area along with total cell area⁶⁵.

Antibodies are an unbound source of potential in the field of cancer therapy⁶⁶. The disturbance of the transferrin receptor 1 (TfR1) may be a way to increase uptake of degraded fragments and ions from these materials⁶⁷. In conjunction with the CuHARs' promising data presented here or other MOBs, a deregulated receptor which has control over iron-based uptake may also be applicable with other metal based materials. With the addition of transferrin, the antibody that stimulates this receptor, there is a possibility to increase the potential influx of anti-cancer metal ions and fragments.

Lastly, I would like to culture cells with CuHARs, adding them at similar doses for both glioma and astrocytes. In contrast to the earlier displayed work provisions would have to be made for cells intended to grow past the normal 90% confluence of a flask (5-9 days), this may be the addition of materials to a cell flask that is raised and passaged, later performing MTT assay on the next "generation" of the cell line. This could also be replicated by plating at a similar cell density in a larger 25ml flask. There, of course, is also the interest in DAPI and calcium imaging on these groups. For calcium imaging, I would expect to see a return to fairly normal response, and with DAPI I suspect for 1-2 cell passage cycles we may see some minor morphology differences indicating stress; but beyond that not much negative impact.

To compound this previous proposed experiment, I would like to add astrocytes to a culture first as they are slower growing. Upon a stable population being achieved, add a fluorescent tracker such as a quantum dot whose fluorescence can sometime be maintained through cell growth periods. A wash would then be performed days later, once the astrocytes had incorporated the particles to remove free floating cells. The culture could then be inoculated with a high dose of similarly labeled glioma, let grow,

washed for dead cells and tracked. A possible treatment would then show a vast reduction in the glioma labeled cells compared to the astrocyte labeled cells using these tracking strategies.

APPENDIX A

ASTROCYTE CULTURE MEDIA

For 250mL total media, use the following amounts:

- 12.5mL Horse serum (5.0%)
- 12.5mL Fetal Bovine Serum (FBS) (0.5%)
- 12.5mL Penicillin/Streptomycin (P/S) (0.5%)
- 223.75mL Ham's F-12K media with L-Glutamine (89.5%)

In a sterile environment, add the component together in the following manner:

1. Add 100mL of Ham's F-12K media to sterile vacuum filtration unit.
2. Add horse serum, FBS, and P/S to vacuum filtration unit.
3. Add 123.5 mL of Ham's F-12K media to unit.
4. Place cap on unit, carefully turn on vacuum.
5. Allow the liquid to pass through the filter, turn off vacuum before bubbles form.
6. Once vacuum is off, remove cap and place screw on cap on the container.
7. Label media including name and date made, store in refrigerator.

APPENDIX B

CRL-2303 CULTURE MEDIA

For 250mL total media, use the following amounts:

- 221.3mL Delbecco Modified Eagle's Medium (DMEM) (88.52%)
- 25mL Fetal Bovine Serum (FBS) (10.0%)
- 1.25mL Penicillin/Streptomycin (P/S) (0.5%)
- 2.5mL Amino Acid Solution (1.0%)

In a sterile environment, add the component together in the following manner:

1. Add 110.65 mL of DMEM to sterile vacuum filtration unit.
2. Add P/S to vacuum filtration unit.
3. Add 25mL FBS to vacuum filtration unit.
4. Add 2.5mL Amino Acid Solution to vacuum filtration unit.
5. Add 110.65 mL of DMEM to sterile vacuum filtration unit.
6. Place cap on unit, carefully turn on vacuum.
7. Allow the liquid to pass through the filter, turn off vacuum before bubbles form.
8. Once vacuum is off, remove cap and place screw on cap on the container.
9. Label media including name and date made, store in refrigerator.

APPENDIX C

POLY-LYSINE PROTOCOL

To coat a dish

1. Use a 1:1 ratio of Poly-lysine to sterile water, or use recycled
2. Use enough mixture to coat the disk/flask and let sit for at least 1 hour at room temp
3. Withdrawal the mixture and store it for future use if it is first batch labeling recycled PLL
4. Wash the flask/dish with PBS 1X and you are ready to plate cells

Important information:

- When poly lysine is sterile, operations should be carried out in the hood.
- The poly-lysine mixture should be stored in a refrigerated environment and can only be reused a single time. Make sure to label (sterile or NS)

APPENDIX D

DAPI STAINING PROTOCOL

Obtain Locke's solution and DAPI aliquots at 14.24 mMol in DI water.

First dilute 3uL of the DAPI stock solution in 297uL of Locke's. Next using the intermedia dilution just created perform a 1:10 with the media in the dish you are staining. For example, if you have 3mL of media in the well of a 12 well plate you will need to add 300uL. Once DAPI has been added incubate the plate at 37°C for 10 minutes and check. Healthier cells may take longer to stain as they will resist the intrusion.

APPENDIX E

MTT ASSAY FOR ASTOCYTES and CRL-2303

It will take 400uL of solution to completely cover the bottom of a 24-well plate. This being considered, 9.6 mL of MTT would be needed to treat an entire plate. 11 ml will be prepared as a safety buffer amount. Similarly, a wash of RPMI is also prepared at 300µL and 7.2mL total 8l safety buffer.

1. Dilute MTT to 5.0mg/ml in RPMI Media the follow a 4x dilution for a final concentration of 1.25mg/ml. for this 13.75mg of MTT powder needs to be added to 11ml of warmed (37°C) RPMI Media.
2. Cell culture Media is removed from cells. A wash of 300uL per well is added and plate gently swirled.
3. Wash solution is removed and 400uL of MTT assay solution is added.
4. Cells are placed back into the incubator at 37* Celsius and incubated at least 1 hr.
5. Cells are removed from incubator and the media is gently removed and discarded
6. 500µL of 91% isopropanol is added to each of the wells and agitated to dissolve the purple crystals. The liquid is removed and placed into individual cuvettes.
7. A pre-warmed spectrophotometer is used and set to blank with 500uL of sterile water. Absorbance is set to 630nm.

APPENDIX F

Standard 7.0 ml Synthesis of MOBs

In sterile conditions

1. Create a solution with a ratio of 7.29mg cysteine to 100 μ l of sterile 1.0 normal sodium hydroxide.
2. Add 7 μ L of the created fresh stock cysteine solution to a T25 flask.
3. Add 6,643 μ L of Sterile water to the flask.
4. Warm in an oven set to 37 °Celsius for 30 minutes.
5. While the flask is warming, prepare a solution of your desired metal such as a pure nanoparticle like copper or a sulfate like CuSO₄ with 2mg/ml in sterile water.
6. Once the flask has warmed, remove and add 350 μ l of your metal solution and place back in the oven to begin synthesis for at least 5 hrs. and up to over night
7. Remove from oven and place in fridge. Micro MOBs should be visible with 10x microscopy.

BIBLIOGRAPHY

1. Karan A, Darder M, Kansakar U, Norcross Z, DeCoster M. Integration of a Copper-Containing Biohybrid (CuHARS) with Cellulose for Subsequent Degradation and Biomedical Control. *Int J Environ Res Public Health*. 2018 Apr 25;15(5):844. doi: 10.3390/ijerph15050844.
2. Ibrahim Khan, Khalid Saeed, Idrees Khan. Nanoparticles: Properties, applications and toxicities. *Arabian Journal of Chemistry*. Volume 12, Issue 7, 2019, Pg. 908-931, ISSN 1878-5352. <https://doi.org/10.1016/j.arabjc.2017.05.011>.
3. Alsaba, M.T., Al Dushaishi, M.F. & Abbas, A.K. A comprehensive review of nanoparticles applications in the oil and gas industry. *J Petrol Explor Prod Technol* **10**, 1389–1399 (2020). <https://doi.org/10.1007/s13202-019-00825-z>
4. Xu L, Liang HW, Yang Y, Yu SH. Stability and Reactivity: Positive and Negative Aspects for Nanoparticle Processing. *Chem Rev*. 2018 Apr 11;118(7):3209-3250. doi: 10.1021/acs.chemrev.7b00208. Epub 2018 Mar 8. PMID: 29517229.
5. F. Sambale, S. Wagner, F. Stahl, R. R. Khaydarov, T. Scheper, D. Bahnemann, "Investigations of the Toxic Effect of Silver Nanoparticles on Mammalian Cell Lines", *Journal of Nanomaterials*, vol. 2015, Article ID 136765, 9 pages, 2015. <https://doi.org/10.1155/2015/136765>
6. Saeed Ahmad Khan. Chapter 1 - Metal nanoparticles toxicity: role of physicochemical aspects. Editor(s): Muhammad Raza Shah, Muhammad Imran, Shafi Ullah. In *Micro and Nano Technologies. Metal Nanoparticles for Drug Delivery and Diagnostic Applications*. Elsevier. 2020. Pg. 1-11. ISBN 9780128169605. <https://doi.org/10.1016/B978-0-12-816960-5.00001-X>.
7. Cotton Kelly, K., Wasserman, J. R., Deodhar, S., Huckaby, J., DeCoster, M. A. Generation of Scalable, Metallic High-Aspect Ratio Nanocomposites in a Biological Liquid Medium. *J. Vis. Exp.* (101), e52901, doi:10.3791/52901 (2015).
8. Jang, N., Kim, B., Lee, G., Lee, H.J., Song, J., & Yun, J.H. Biological synthesis of copper nanoparticles using plant extract. *Semantic Scholar* (2011).

9. PRABHU BM, ALI SF, MURDOCK RC, HUSSAIN SM, SRIVATSAN M. Copper nanoparticles exert size and concentration dependent toxicity on somatosensory of rat. *Nanotoxicology* 4 (2): 150-160, 2010.
10. Javid Muhammad Arshad, Waleed Rāza, Niama Amin, Khalid Nadeem, M. Imran Arshad, M. Azhar Khan. Synthesis and characterization of cobalt ferrites as MRI contrast agent. *Materials Today: Proceedings*. 2020. bISSN 2214-7853. <https://doi.org/10.1016/j.matpr.2020.04.746>.
11. Geng P, Zhang X, Teng Y, Fu Y, Xu L, Xu M, Jin L, Zhang W. A DNA sequence-specific electrochemical biosensor based on alginate-coated cobalt magnetic beads for the detection of *E. coli*. *Biosens Bioelectron*. 2011 Mar 15;26(7):3325-30. doi: 10.1016/j.bios.2011.01.007.
12. Rauwel E, Al-Arag S, Salehi H, Amorim CO, Cuisinier F, Guha M, Rosario MS, Rauwel P. Assessing Cobalt Metal Nanoparticles Uptake by Cancer Cells Using Live Raman Spectroscopy. *Int J Nanomedicine*. 2020 Sep 24; 15:7051-7062. doi: 10.2147/IJN.S258060.
13. Frickenstein, Alex N et al. "Mesoporous Silica Nanoparticles: Properties and Strategies for Enhancing Clinical Effect." *Pharmaceutics* vol. 13,4 570. 17 Apr. 2021, doi:10.3390/pharmaceutics13040570
14. Ng CT, Yong LQ, Hande MP, Ong CN, Yu LE, Bay BH, Baeg GH. Zinc oxide nanoparticles exhibit cytotoxicity and genotoxicity through oxidative stress responses in human lung fibroblasts and *Drosophila melanogaster*. *Int J Nanomedicine*. 2017 Feb 28; 12:1621-1637. doi: 10.2147/IJN.S124403.
15. Ostrovsky, S., Kazimirsky, G., Gedanken, A. *et al.* Selective cytotoxic effect of ZnO nanoparticles on glioma cells. *Nano Res.* 2, 882–890 (2009). <https://doi.org/10.1007/s12274-009-9089-5>
16. Grass, Gregor et al. "Metallic copper as an antimicrobial surface." *Applied and environmental microbiology* vol. 77,5 (2011): 1541-7. doi:10.1128/AEM.02766-10
17. Longano, Daniela et al. "Synthesis and Antimicrobial Activity of Copper Nanomaterials." *Nano-Antimicrobials: Progress and Prospects* 85–117. 26 Aug. 2011, doi:10.1007/978-3-642-24428-5_3

18. Ermini, Maria Laura, and Valerio Voliani. "Antimicrobial Nano-Agents: The Copper Age." *ACS nano* vol. 15,4 (2021): 6008-6029.
doi:10.1021/acsnano.0c10756
19. Wang Y, Zhao Q, Han N, Bai L, Li J, Liu J, Che E, Hu L, Zhang Q, Jiang T, Wang S. Mesoporous silica nanoparticles in drug delivery and biomedical applications. *Nanomedicine*. 2015 Feb;11(2):313-27. doi: 10.1016/j.nano.2014.09.014.
20. Clemente Plaza, Noelia et al. "Effects of the Usage of l-Cysteine (l-Cys) on Human Health." *Molecules (Basel, Switzerland)* vol. 23,3 575. 3 Mar. 2018, doi:10.3390/molecules23030575
21. Gortner, R. A.; Hoffman, W. F. (1925). "L-Cystine". *Organic Syntheses*. 5: 39.
22. Bergweft, H. MolView.org. GPLI software. 2015.
23. Mandal, Nabarun et al. "Effect of Copper on l-Cysteine/l-Cystine Influx in Normal Human Erythrocytes and Erythrocytes of Wilson's Disease." *Indian journal of clinical biochemistry: IJCB* vol. 31,4 (2016): 468-72.
doi:10.1007/s12291-016-0555-z
24. Copper binding by a unique family of metalloproteins is dependent on kynurenine formation. Anastasia C. Manesis, Richard J. Jodts, Brian M. Hoffman, Amy C. Rosenzweig. *Proceedings of the National Academy of Sciences* July. 2021, 118 (23) e2100680118; DOI: 10.1073/pnas.2100680118
25. Banci L., Bertini I. (2013) *Metallomics and the Cell: Some Definitions and General Comments*. In: Banci L. (eds) *Metallomics and the Cell. Metal Ions in Life Sciences*, vol 12. Springer, Dordrecht. https://doi.org/10.1007/978-94-007-5561-1_1
26. Ranjita Shegokar, Mostafa Nakach. Chapter 4 - Large-scale manufacturing of nanoparticles—An industrial outlook. *Drug Delivery Aspects*. Elsevier. 2020. Pg 57-77. ISBN 9780128212226. <https://doi.org/10.1016/B978-0-12-821222-6.00004-X>.
27. Paliwal, R., Babu, R.J. & Palakurthi, S. Nanomedicine Scale-up Technologies: Feasibilities and Challenges. *AAPS PharmSciTech* **15**, 1527–1534 (2014). <https://doi.org/10.1208/s12249-014-0177-9>

28. Fischer, N. W. (1831). "Ueber Stickstoffoxyd-Salze". *Annalen der Physik und Chemie*. **97** (1): 160–163. Bibcode:1831AnP....97..160F. doi:10.1002/andp.18310970114
29. Rigo A et al. Interaction of copper with cysteine: stability of cuprous complexes and catalytic role of cupric ions in anaerobic thiol oxidation. *Journal of Inorganic Biochemistry*. Vol 98, Issue 9. 2004. Pg 1495-1501. ISSN 0162-0134. <https://doi.org/10.1016/j.jinorgbio.2004.06.008>.
30. Anderson, Richard C et al. "Changes in the immunologic phenotype of human malignant glioma cells after passaging in vitro." *Clinical immunology (Orlando, Fla.)* vol. 102,1 (2002): 84-95. doi:10.1006/clim.2001.5152
31. Higgins, Dominique M et al. "Brain tumor stem cell multipotency correlates with nanog expression and extent of passaging in human glioblastoma xenografts." *Oncotarget* vol. 4,5 (2013): 792-801. doi:10.18632/oncotarget.1059
32. Passaquin, A.-C., Schreier, W.A. and de Vellis, J. (1994), Gene expression in astrocytes is affected by subculture. *International Journal of Developmental Neuroscience*, 12: 363-372. [https://doi.org/10.1016/0736-5748\(94\)90086-8](https://doi.org/10.1016/0736-5748(94)90086-8)
33. Spring Harbour Protocol 2006. PBS Phosphate Buffered Saline. 2006. Cold Spring Harbor Laboratory Press doi: 10.1101/pdb.rec8247Cold
34. "Trypsin-EDTA (0.25%)". Stem Cell Technologies. Retrieved 2021-11-7.
35. Stemcell.com. 2021. *Counting Cells with a Hemocytometer*. [online] Available at: <<https://www.stemcell.com/how-to-count-cells-with-a-hemocytometer.html>> [Accessed 8 November 2021].
36. Allevi. 2021. *Passaging Cells (General)*. [online] Available at: <<https://www.allevi3d.com/passaging-cells-protocol/>> [Accessed 8 November 2021].
37. Haenel, F. Garbow, N. "Cell Counting and Confluency Analysis as Quality Controls in Cell-Based Assays" online Cell Counting and Confluency Analysis as Quality Controls in Cell-Based Assays (perkinelmer.com) Retrieved 2021-11-7

38. Jing Wang, Lingling Tian, Nuan Chen, Seeram Ramakrishna, Xiumei Mo. The cellular response of nerve cells on poly-l-lysine coated PLGA-MWCNTs aligned nanofibers under electrical stimulation. *Materials Science and Engineering: C*. Vol. 91. 2018. Pg 715-726. ISSN 0928 4931. <https://doi.org/10.1016/j.msec.2018.06.025>.
39. Van Meerloo, Johan et al. "Cell sensitivity assays: the MTT assay." *Methods in molecular biology* (Clifton, N.J.) vol. 731 (2011): 237-45. doi:10.1007/978-1-61779-080-5_20
40. Stemcell.com. 2021. *Counting Cells with a Hemocytometer*. [online] Available at: <<https://www.stemcell.com/how-to-count-cells-with-a-hemocytometer.html>> [Accessed 8 November 2021].
41. Liu, Y et al. "Mechanism of cellular 3-(4,5-dimethylthiazol-2-yl)-2,5-diphenyltetrazolium bromide (MTT) reduction." *Journal of neurochemistry* vol. 69,2 (1997): 581-93. doi:10.1046/j.1471-4159.1997.69020581.x
42. "Locke's solution." *Miller-Keane Encyclopedia and Dictionary of Medicine, Nursing, and Allied Health, Seventh Edition*. 2003. Saunders, an imprint of Elsevier, Inc 7 Nov. 2021 <https://medical-dictionary.thefreedictionary.com/Locke%27s+solution>
43. Tharmalingam, T et al. "Pluronic enhances the robustness and reduces the cell attachment of mammalian cells." *Molecular biotechnology* vol. 39,2 (2008): 167-77. doi:10.1007/s12033-008-9045-8
44. Gee KR, Brown KA, Chen WN, Bishop-Stewart J, Gray D, Johnson I (February 2000). "Chemical and physiological characterization of fluo-4 Ca(2+)-indicator dyes". *Cell Calcium*. **27** (2): 97–106. doi:10.1054/ceca.1999.0095. PMID 10756976.
45. Cherry, R.S. and Papoutsakis, E.T. (1988), Physical mechanisms of cell damage in microcarrier cell culture bioreactors. *Biotechnol. Bioeng.*, 32: 1001-1014. <https://doi.org/10.1002/bit.260320808>
46. Kapuscinski, J. (September 1995). "DAPI: a DNA-specific fluorescent probe". *Biotech. Histochem.* **70** (5): 220–233. doi:10.3109/10520299509108199. PMID 8580206

47. Kapuscinski, J (2017). "Interactions of nucleic acids with fluorescent dyes: spectral properties of condensed complexes". *Journal of Histochemistry & Cytochemistry*. **38** (9): 1323–1329. doi:10.1177/38.9.1696951. PMID 1696951.
48. Watanabe W, Konno K, Ijichi K, Inoue H, Yokota T, Shigeta S. MTT colorimetric assay system for the screening of anti-orthomyxo- and anti-paramyxoviral agents. *J Virol Methods*. 1994 Jul;48(2-3):257-65. doi: 10.1016/0166-0934(94)90124-4.
49. Garini, Y et al. "Signal to noise analysis of multiple color fluorescence imaging microscopy." *Cytometry* vol. 35,3 (1999): 214-26. doi:10.1002/(sici)1097-0320(19990301)35:3<214::aid-cyto4>3.0.co;2-d
50. Ettinger, Andreas, and Torsten Wittmann. "Fluorescence live cell imaging." *Methods in cell biology* vol. 123 (2014): 77-94. doi:10.1016/B978-0-12-420138-5.00005-7
51. Baba AI, Cătoi C. Comparative Oncology. Bucharest (RO): The Publishing House of the Romanian Academy; 2007. Chapter 3, TUMOR CELL MORPHOLOGY. Available from: <https://www.ncbi.nlm.nih.gov/books/NBK9553/>
52. Chazotte B. Labeling nuclear DNA using DAPI. *Cold Spring Harb Protoc*. 2011 Jan 1;2011(1):pdb.prot5556. doi: 10.1101/pdb.prot5556.
53. Khezerlou, Elnaz & Prajapati, Neela & DeCoster, Mark. (2021). Negative Feedback Role of Astrocytes in Shaping Excitation in Brain Cell Co-cultures. *Frontiers in Cellular Neuroscience*. 15. 10.3389/fncel.2021.651509.
54. Romera-Cárdenas G, Thomas LM, Lopez-Cobo S, García-Cuesta EM, Long EO, et al. (2016) Ionomycin Treatment Renders NK Cells Hyporesponsive. *PLOS ONE* 11(3): e0150998. <https://doi.org/10.1371/journal.pone.0150998>
55. Morgan AJ, Jacob R. Ionomycin enhances Ca²⁺ influx by stimulating store-regulated cation entry and not by a direct action at the plasma membrane. *Biochem J*. 1994 Jun 15;300 (Pt 3)(Pt 3):665-72. doi: 10.1042/bj3000665.
56. DeCoster, Mark. (2007). The Nuclear Area Factor (NAF): a measure for cell apoptosis using microscopy and image analysis.

57. Suresh Kumar Kailasa, Madhurya Chandel, Vaibhavkumar N. Mehta, Tae Jung Park. Influence of ligand chemistry on silver nanoparticles for colorimetric detection of Cr³⁺ and Hg²⁺ ions. *Spectrochimica Acta Part A: Molecular and Biomolecular Spectroscopy*. V 195.2018.Pg 120-127. ISSN 1386-1425. <https://doi.org/10.1016/j.saa.2018.01.038>.
58. Di Bucchianico S, Fabbrizi MR, Misra SK, Valsami-Jones E, Berhanu D, Reip P, Bergamaschi E, Migliore L. Multiple cytotoxic and genotoxic effects induced in vitro by differently shaped copper oxide nanomaterials.
59. Cassandri, M., Smirnov, A., Novelli, F. *et al.* Zinc-finger proteins in health and disease. *Cell Death Discov.* **3**, 17071 (2017). <https://doi.org/10.1038/cddiscovery.2017.71>
60. Roohani, N. *et al.* "Zinc and its importance for human health: An integrative review." *Journal of research in medical sciences: the official journal of Isfahan University of Medical Sciences* vol. 18,2 (2013): 144-57.
61. Park, K.H., Park, B., Yoon, D.S. *et al.* Zinc inhibits osteoclast differentiation by suppression of Ca²⁺-Calcineurin-NFATc1 signaling pathway. *Cell Commun Signal* **11**, 74 (2013). <https://doi.org/10.1186/1478-811X-11-74>
62. A. Gilardino *et al.* Interaction of SiO₂ nanoparticles with neuronal cells: Ionic mechanisms involved in the perturbation of calcium homeostasis. *The International Journal of Biochemistry & Cell Biology*. Vol. 66. 2015. Pg 101-111. ISSN 1357-2725. <https://doi.org/10.1016/j.biocel.2015.07.012>.
63. Chekhonin, Ivan V *et al.* "Glioma Cell and Astrocyte Co-cultures As a Model to Study Tumor-Tissue Interactions: A Review of Methods." *Cellular and molecular neurobiology* vol. 38,6 (2018): 1179-1195. doi:10.1007/s10571-018-0588-3
64. Culotta E, Koshland DE Jr. NO news is good news. *Science*. 1992 Dec 18;258(5090):1862-5. doi: 10.1126/science.1361684. PMID: 1361684.
65. Silverman, J.F. and Frable, W.J. (1990), The use of the diff-quick stain in the immediate interpretation of fine-needle aspiration biopsies. *Diagn. Cytopathol.*, 6: 366-369. <https://doi.org/10.1002/dc.2840060516>.

66. Baek, Taehwa et al. "Image analytic study of nuclear area in mantle cell lymphoma." *The Korean journal of hematology* vol. 45,3 (2010): 193-6. doi:10.5045/kjh.2010.45.3.193
67. Scott AM, Wolchok JD, Old LJ. Antibody therapy of cancer. *Nat Rev Cancer*. 2012 Mar 22;12(4):278-87. doi: 10.1038/nrc3236. PMID: 22437872.
68. Candelaria, Pierre V et al. "Antibodies Targeting the Transferrin Receptor 1 (TfR1) as Direct Anti-cancer Agents." *Frontiers in immunology* vol. 12 607692. 17 Mar. 2021, doi:10.3389/fimmu.2021.607692